Biofísica 2015

Laboratorio 2: Elastómeros

Primera parte: Módulo de Young de un polímero

La elasticidad de un material polimérico está formada por la contribución elástica de cada una de las subcadenas que constituyen al material. Una subcadena es la porción de polímero comprendida entre dos entrecruzamientos. Un entrecruzamiento es la unión química que se establece, durante el proceso de vulcanización, entre puntos diferentes de una misma cadena o cadenas diferentes.

Consideremos un cuerpo sólido, altamente elástico, constituido por un material polimérico (como por ejemplo, una pelota de caucho). Las macromoléculas que constituyen al material están considerablemente empaquetadas e interactúan fuertemente entre sí, pero es posible considerar a cada subcadena como un polímero ideal, sin interacciones por volumen excluido. En esa densa estructura, el movimiento térmico de las moléculas es equivalente al de un ovillo estadístico ideal ("random coil" o cadena aleatoria). Los grupos atómicos que constituyen un monómero oscilan y rotan en un modo independiente entre sí, de modo que las dimensiones lineales de cada subcadena sigue siendo proporcional a la raíz cuadrada de su longitud química o longitud de contorno.

De modo tal que trataremos a nuestro material polimérico en estudio, como a un conjunto de subcadenas ideales. Supongamos entonces que cada cadena está formada por **N** segmentos libremente articulados, cada uno de longitud **l** (para simplificar, omitimos la polidispersidad del polímero). Cuando el material es estirado, todas sus subcadenas sufren, en promedio, el mismo estiramiento. La entropía de cada subcadena disminuye a medida que su distancia entre extremos **h** aumenta. Este es el origen entrópico de la fuerza elástica, pero no explica la alta elasticidad. Esta propiedad se define como la capacidad del material de sufrir una alta deformación reversible cuando se lo somete a una tensión moderada, y es debido a que el módulo elástico de cada cadena es relativamente pequeño.

Por razones de simplicidad, consideremos una porción de material con forma de paralelepípedo rectangular y un sistema de coordenadas cartesiano a lo largo de sus aristas. Supongamos que hemos elongado el material en factores λ_x, λ_y, λ_z, a lo largo de cada uno de sus ejes y que el vector distancia entre extremos de una cierta subcadena era inicialmente h_o con componentes $\mathbf{h_{ox}}$, $\mathbf{h_{oy}}$ y $\mathbf{h_{oz}}$. Luego de la deformación el vector distancia entre extremos será h y sus componentes serán $\lambda_x\mathbf{h_{ox}}$, $\lambda_y\mathbf{h_{oy}}$ y $\lambda_z\mathbf{h_{oz}}$. El cambio de entropía que experimenta cada subcadena será:

$$\Delta S(\mathbf{h}) = S(h) - S(ho) = - 3k\,[(\mathbf{h_x} - \mathbf{h_{ox}}^2) + (\mathbf{h_y} - \mathbf{h_{oy}}^2) + (\mathbf{h_z} - \mathbf{h_{oz}}^2)]\,/2\,N\,\mathbf{l}^2$$

$$= - 3k\,[(\lambda_x^2-1)\,\mathbf{h_{ox}}^2 + (\lambda_y^2-1)\,\mathbf{h_{oy}}^2 + (\lambda_z^2-1)\,\mathbf{h_{oz}}^2]\,/2\,N\,\mathbf{l}^2$$

Para encontrar el cambio total de entropía de la red, formada por todas las subcadenas, debemos sumar la ecuación anterior para todas las subcadenas. Es decir, podemos promediar sobre **ho** y luego multiplicar por el numero de subcadenas, vV, que hay en la red, en donde V es el volumen de la muestra, y v es la concentración de subcadenas por unidad de volumen.

$\Delta S(\mathbf{h}) = - 3kvV \; [(\lambda_x^2-1) \langle \mathbf{h_{ox}^2} \rangle + (\lambda_y^2-1) \langle \mathbf{h_{oy}^2} \rangle + (\lambda_z^2-1) \langle \mathbf{h_{oz}^2} \rangle] /2 \, N \, \mathbf{l}^2$.

Teniendo en cuenta que:

$\langle \mathbf{h_o^2} \rangle = \langle \mathbf{h_{ox}^2} \rangle + \langle \mathbf{h_{oy}^2} \rangle + \langle \mathbf{h_{oz}^2} \rangle$.

Luego, las tres direcciones son equivalentes, por lo tanto:

$\langle \mathbf{h_{ox}^2} \rangle = \langle \mathbf{h_{oy}^2} \rangle = \langle \mathbf{h_{oz}^2} \rangle = N \, \mathbf{l}^2 /3$.

Finalmente se obtiene:

$\Delta S = -kvV \, (\lambda_x^2+\lambda_y^2+\lambda_z^2-3) /2$.

Es importante notar que el resultado es independiente de los parámetros N y **l** que describen individualmente a una subcadena, de modo que la última ecuación es universal.

Supongamos ahora que hemos elongado la muestra en un factor λ a lo largo del eje x, es decir, $\lambda_x = \lambda$. y el volumen de la muestra no ha cambiado a causa del estiramiento, ya que estamos tratando un material altamente elástico. Entonces:

$\lambda_y = \lambda_z = \lambda^{-1/2}$

Por ende, el volumen total luego de la deformación, V, es igual al volumen inicial. Evidentemente, un polímero se comporta en forma diferente a un cristal sólido ordinario. En un cristal, el cambio de volumen se produce por un cambio en las posiciones de sus átomos. Un polímero aumenta su longitud al desenrollarse sus subcadenas, mientras que las distancias entre sus átomos se mantienen constantes. Sustituyendo se obtiene:

$\Delta S = -kvV \, (\lambda^3+2/\lambda-3) /2$.

La fuerza de estiramiento será:

$f= -T \, \Delta S/\Delta a_x = -(T/a_{ox}) \, (\Delta S/\Delta \lambda) = -(T/a_{ox}) \, (\delta S/\delta\lambda)$.

Como estamos interesados en la tensión, definida como la fuerza por unidad de área transversal inicial ($a_{oy} \, a_{oz}$):

$\sigma = f / (a_{oy} \, a_{oz}) = - [T/(a_{ox} \, a_{oy} \, a_{oz})] \, (\delta S/\delta\lambda) = - [T/V] \, (\delta S/\delta\lambda)$.

Por lo tanto,

$\sigma = kTv\ (\lambda - 1/\lambda^2)$.

Si la elongación es pequeña ($\lambda \approx 1$), esta ecuación se puede usar para estimar el modulo de Young de un material polimérico, de la forma

$\sigma \approx 3kTv\ (\lambda - 1)$.

El término entre paréntesis representa la elongación relativa, $\Delta a_x/a_{ox}$. El módulo de Young, E, se define como el cociente entre la tensión y la elongación relativa:

$E = 3kTv$.

Protocolo Experimental

i) Una muestra de material polimérico, a una temperatura T_1, se somete a diferentes tensiones y se determina la elongación relativa λ para cada caso.

ii) Mediante el gráfico σ vs $(\lambda-1)$, para valores de λ cercanos a uno, se estima el módulo de Young (E) a una temperatura T_1.

iii) Un grafico σ vs $\lambda - 1/\lambda^2$ permite estimar el valor de λ hasta el cual las hipótesis del modelo se cumplen razonablemente bien.

iv) Se repite el procedimiento a una temperatura T_2.

v) Verifique si las pendientes de los gráficos ii) a T1 y T2 cumplen la relación teórica:

Pendiente (T_1) / Pendiente (T_2) = T_1 / T_2

vi) Ídem con gráficos iii).

vii) Calcule a partir del valor de las pendientes encontradas el número de entrecruzamientos por unidad de volumen, V.

viii) Estime la densidad del material utilizado.

ix) A partir de los datos hallados en vii) y viii) estime el peso molecular promedio de las subunidades que constituyen el material en estudio.

Segunda parte: Reticulación (‘Cross-link’) en tejidos biológicos

La reticulación implica la formación de una red tridimensional formada por la unión de las diferentes cadenas poliméricas homogéneas. A partir de las publicaciones adjuntadas, discutir la relación del módulo de Young (y la capacidad de soportar esfuerzo) con el grado de reticulación en un material elastomérico, en este caso un tendón (donde el polímero que entrecruza es el colágeno).

Experimental Diab. Res., 5:143–153, 2004
ISSN: 1543-8600 print / 1543-8619 online
DOI: 10.1080/15438600490277860

Taylor & Francis
Taylor & Francis Group

Cross-Linking in Collagen by Nonenzymatic Glycation Increases the Matrix Stiffness in Rabbit Achilles Tendon

G. Kesava Reddy

Department of Physical Therapy and Rehabilitation Sciences, University of Kansas Medical Center, Kansas City, Kansas, USA

Nonenzymatic glycation of connective tissue matrix proteins is a major contributor to the pathology of diabetes and aging. Previously the author and colleagues have shown that nonenzymatic glycation significantly enhances the matrix stability in the Achilles tendon (Reddy et al., 2002, *Arch. Biochem. Biophys.*, 399, 174–180). The present study was designed to gain further insight into glycation-induced collagen cross-linking and its relationship to matrix stiffness in the rabbit Achilles tendon. The glycation process was initiated by incubating the Achilles tendons (n = 6) in phosphate-buffered saline containing ribose, whereas control tendons (n = 6) were incubated in phosphate-buffered saline without ribose. Eight weeks following glycation, the biomechanical attributes as well as the degree of collagen cross-linking were determined to examine the potential associations between matrix stiffness and molecular properties of collagen. Compared to nonglycated tendons, the glycated tendons showed increased maximum load, stress, strain, Young's modulus of elasticity, and toughness indicating that glycation increases the matrix stiffness in the tendons. Glycation of tendons resulted in a considerable decrease in soluble collagen content and a significant increase in insoluble collagen and pentosidine. Analysis of potential associations between the matrix stiffness and degree of collagen cross-linking showed that both insoluble collagen and pentosidine exhibited a significant positive correlation with the maximum load, stress, and strain, Young's modulus of elasticity, and toughness (*r* values ranging from .61 to .94) in the Achilles tendons. However, the soluble collagen content present in neutral salt buffer, acetate buffer, and acetate buffer containing pepsin showed an inverse relation with the various biomechanical attributes tested (*r* values ranging from .22 to .84) in the Achilles tendons. The results of the study demonstrate that glycation-induced collagen cross-linking is directly associated with the increased matrix stiffness and other mechanical attributes of the tendon.

Keywords Collagen Cross-Linking; Connective Tissue Matrix; Glycation; Maillard Reaction; Stiffness; Tissue Biomechanics

Nonenzymatic glycation, also known as the Maillard reaction between reducing sugars and proteins, contributes to the chemical aging of tissue proteins in vivo and to the accelerated aging of proteins in diabetes mellitus [1–3]. In this reaction, sugars react reversibly with the free amino group of proteins to form unstable Schiff bases, which then undergo an intramolecular rearrangement to form a stable Amadori product [4, 5]. These Amadori products are believed to undergo a series of reactions to form heterogeneous complex fluorophores and chromophores collectively referred to as advanced Maillard products or advanced glycation end products (AGEs). The production of these AGE products have been implicated in the etiology of the long-term complications of several human afflictions, such as diabetes [1, 3, 6], aging [7], atherosclerosis [8], fibromyalgia [9], uremia [10, 11], Alzheimer's disease [12, 13], and renal failure [14].

Collagen provides many basic functional attributes of the connective tissues in the body. Glycation can affect collagen in a number of ways: its ability to form precise supramolecular aggregates, the alterations in its charge profile, defects in the

Received 29 June 2003; accepted 11 September 2003.
These studies were supported by a grant from the American Heart Association, the Heartland Affiliate Research Program (AHA-9960226Z), to GKR.
Address correspondence to Dr. G. Kesava Reddy, Baylor-Sammons Cancer Center, Suite 185, 3535 Worth Street, Dallas, TX 75246, USA. E-mail: kreddy@yahoo.com

formation of its fibrils, and hence its interaction with cells. In addition to the occurrence of biochemical and morphological manifestations, glycation has been shown to alter the biomechanical functioning of the connective tissues [15–21]. Both in vivo and in vitro studies have shown that reducing sugars, such as glucose and ribose, react with the amino groups of collagen and other proteins and form cross-linked AGEs in the tissue. These AGEs accumulate over time and lead to the functional impairment of the tissue. Earlier studies have shown that glycation alters the structural properties of collagen [22]. These earlier studies investigated the effect of glycation on either the biochemical nature of collagen or the biomechanical functions of the tissue. However, the interrelationship between the altered biochemical properties of collagen and the altered biomechanical functions of the tendon produced by glycation requires further investigation.

Despite recent advances in our understanding of glycation of proteins, there is relatively little evidence available concerning the glycation-induced collagen cross-linking that is directly responsible for the altered stiffness of the tissue. Recently, we have shown that nonenzymatic glycation alters both biomechanical and biochemical functioning of the connective tissue matrix in rabbit Achilles tendon [23]. In the present study, we report a direct analysis of the potential associations between the degree of collagen cross-linking and matrix stiffness in Achilles tendon following nonenzymatic glycation.

MATERIALS AND METHODS

Achilles tendons from white male New Zealand rabbits, aged 12 to 16 weeks, were collected and stored at −70°C. The procedures for tendon excision were described in detail previously [23–26].

Glycation of Achilles Tendons With Ribose

The details of the glycation of Achilles tendons with ribose were described previously [23]. Briefly, at the start of the experiment, the tendons were thawed at room temperature and washed extensively in 20 mM phosphate-buffered saline (PBS), pH 7.4, containing 0.1% sodium azide as preservative. The specimens were divided equally into control (nonglycated) and experimental (glycated) groups (n = 6 per group) by random selection. The glycation process was initiated by incubating the tissue specimens with 0.2 M ribose in PBS, pH 7.4, containing 0.1% sodium azide. The tendons in the control group were incubated in PBS, pH 7.4, containing 0.1% sodium azide without ribose. The nonenzymatic glycation reaction process was allowed to proceed for 8 weeks at 29°C ± 1°C in a temperature-controlled incubator. During the initial 2 weeks, the incubation medium was changed for all samples every 3rd day. Subsequently the medium was changed every 4th day.

Biomechanical Analysis

The analysis of the biomechanical properties of tendons was carried out using the Instron Materials Testing Device, Model 8511 (Instron, Canton, MA) as described extensively in our previous work [23, 24, 26]. Initially, the tendon specimens were secured between the clamps and pulled to rupture at a crosshead speed of 250 mm/min. The data were digitized, displayed, and a load versus displacement curve was recorded using an IBM computer. From the load/deformation curve, tensile strength, stress, strain, Young's modulus of elasticity, and toughness were calculated for each specimen.

Biochemical Analyses

Immediately following biomechanical measurements, the ruptured Achilles tendons were collected and used for biochemical analysis. The failure site of the tendons (site of rupture) was dissected from each tendon, cut into fine pieces, and processed for biochemical analysis.

Determination of the Degree of Collagen Cross-Linking

The extent of collagen cross-linking was assessed by sequential extractions of collagen in neutral salt buffer, acetate buffer, and acetate buffer containing pepsin as described earlier

TABLE 1
Comparison of various biomechanical characteristics of control and glycated rabbit Achilles tendons

Biomechanical measurements	Control Achilles tendon	Glycated Achilles tendon	Change (%)
Maximum load (N)	292.30 ± 9.8	438.03 ± 20.95*	+50
Maximum stress (MPa)	7.83 ± 0.51	20.25 ± 2.13*	+159
Maximum strain (%)	59.59 ± 3.21	68.51 ± 2.93*	+15
Young's modulus (MPa)	24.89 ± 1.52	65.087 ± 14.41*	+161
Energy absorption (mJ)	392.30 ± 51.54	1038.32 ± 109.35*	+164
Toughness (MPa)	4.92 ± 0.65	13.58 ± 1.2563*	+176

Note. Values are mean ± SE (N = 6).
*$P < .001$.

TABLE 2
Comparison of various biomechanical characteristics at breakpoint of control and glycated rabbit Achilles tendons

Biomechanical measurements	Control Achilles tendon	Glycated Achilles tendon	Change (%)
Load at break (N)	125.25 ± 9.90	147.66 ± 4.60*	+18
Stress at break (MPa)	3.45 ± 0.28	6.29 ± 0.43*	+80
Strain at break (%)	118.49 ± 7.90	126.96 ± 7.40	+8
Energy absorption at break (mJ)	245.40 ± 18.60	280.09 ± 16.02	+14

Note. Values are mean ± SE (N = 6).
*$P < .001$.

[24, 25]. In addition, the glycation-induced cross-linking was determined using pentosidine assay as described previously [23].

Hydroxyproline Assay

The methods used to quantify the amount of hydroxyproline present in neutral salt soluble collagen (NSC), acid soluble collagen (ASC), pepsin soluble collagen (PSC), and insoluble collagen (ISC) have been extensively described in our previous work [23–25, 27]. Briefly, aliquots of the samples were hydrolyzed in alkali and oxidized with chloramine-T. The chromophore was developed with the addition of Ehrlich's aldehyde and the absorbance of the chromophore was measured at 550 nm. Unknown concentrations of hydroxyproline in each tissue specimen were deduced from a standard calibration curve. The total collagen content was calculated assuming that hydroxyproline comprises 14% of the total amino acids of collagen.

Quantitation of Pentosidine

The measurement of pentosidine levels in glycated and nonglycated tendons was determined using a previously reported procedure [23, 28], employing high-performance liquid chromatography (HPLC; Shimadzu) with a binary gradient system module managing a RF-10A spectrofluorometric detector. Briefly, both glycated and nonglycated samples were hydrolyzed in 6 N HCl for 16 hours at 110°C and freeze-dried to remove the acid. They were then reconstituted in distilled water, aliquots were taken into 0.1% trifluoroacetic acid (TFA), and analyzed by HPLC using a C18 reverse-phase column (Supelco Supelcosil 25 cm × 4.6 mm with 5-mm LC-18 pore size) equilibrated with 0.1% TFA. A gradient of 0% to 6% acetonitrile (0.1% in TFA) was run in 30 minutes at a flow rate of about 1 mL per minute. A standard curve was generated by running known quantities of pentosidine (kindly provided by Dr. Raja Khalifah) using 335 nm excitation/385 nm emission fluorescence. Elution position and the amount of fluorescence was compared to the pentosidine standard for quantitation.

Statistical Analysis

The results were expressed as a mean ± standard error. Statistical significances of the differences between the nonglycated and glycated Achilles tendons were evaluated using 1-way analysis of variance (ANOVA). Using Sigmastat software, a linear regression analysis was performed to correlate biochemical and biomechanical measurements. A P value less than .05 was considered statistically significant.

RESULTS

Biomechanical Measurements

The biomechanical tests indicated significant differences in biomechanical properties between the nonglycated and glycated Achilles tendons (Tables 1 and 2). Measurements of

TABLE 3
Comparison of the degree of collagen cross-linking between the control and glycated rabbit Achilles tendons

Degree of collagen cross-linking	Control Achilles tendon	Glycated Achilles tendon	Change (%)
Neutral salt soluble collagen (NSC)[a]	4.40 ± 0.52	2.71 ± 0.26*	−61
Acid soluble collagen (ASC)[a]	15.61 ± 0.86	8.40 ± 0.52*	−48
Pepsin soluble collagen (PSC)[a]	178.60 ± 7.90	112.60 ± 4.7*	−29
Insoluble collagen (ISC)[a]	332.00 ± 16.10	426.50 ± 13.06*	+28
Pentosidine[b]	2.20 ± 0.20	5.90 ± 0.30*	+168

Note. Values are mean ± SE (N = 6).
[a]Expressed as μg/mg of dry tissue.
[b]Expressed as pmol/mg of collagen.
*$P < .001$.

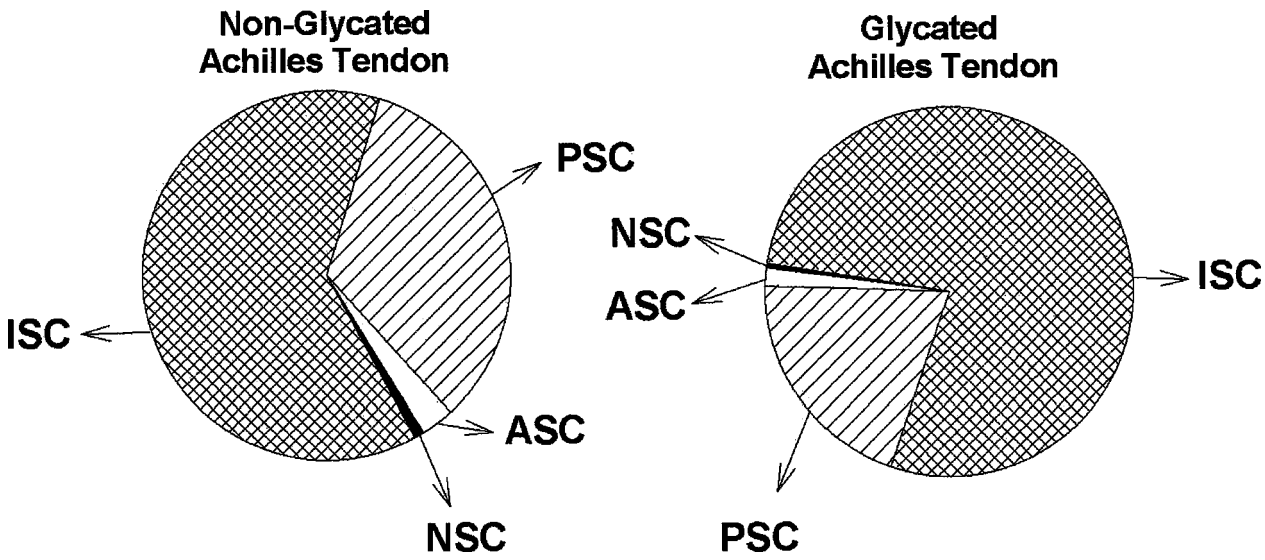

FIGURE 1
The distribution of the relative proportions of neutral salt soluble, acid soluble, pepsin soluble, and insoluble collagens in nonglycated and glycated Achilles tendons.

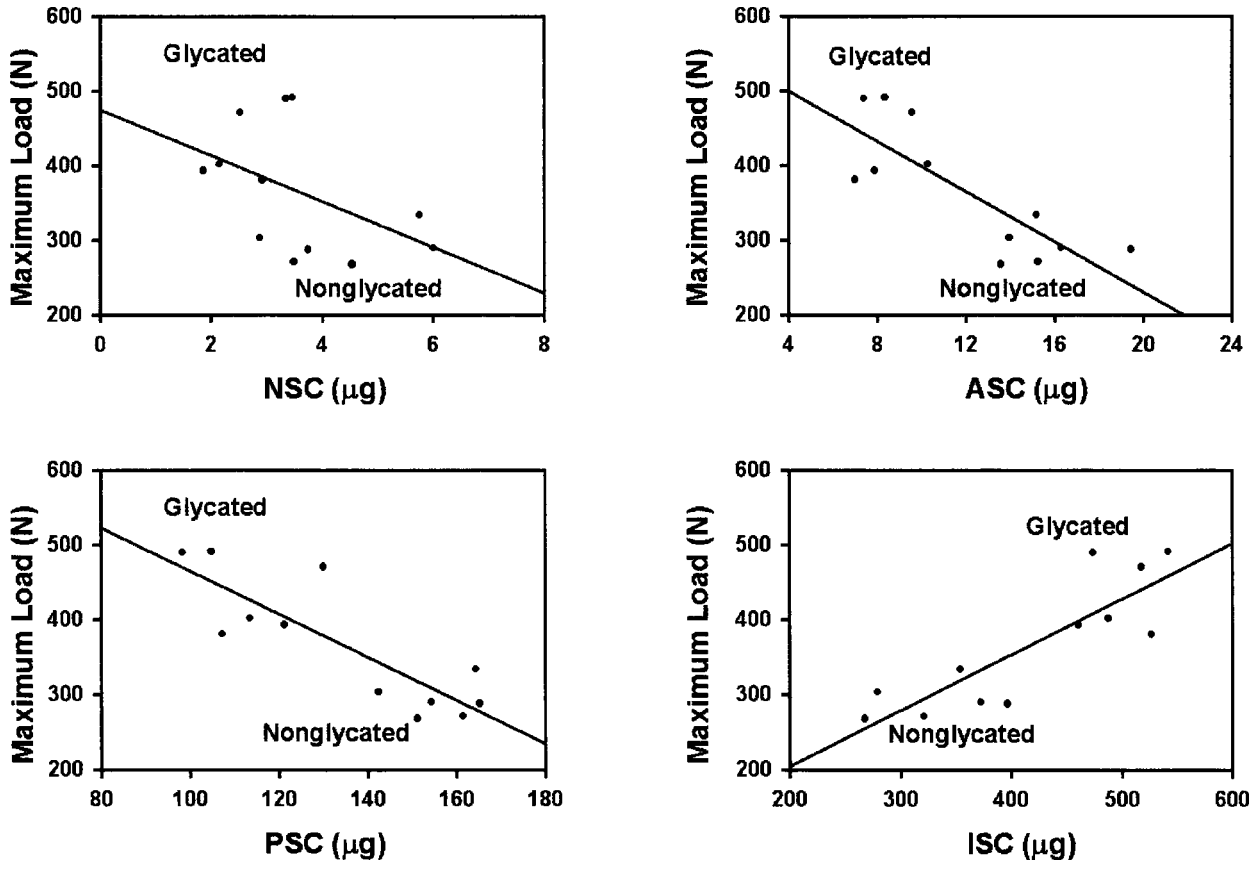

FIGURE 2
Scatterplots illustrating the correlation between maximum load and soluble and insoluble collagen contents from glycated and nonglycated tendons. Regression analysis showed that the maximum load of the tendons inversely correlated with the NSC ($r = .47$, $P < .01$), ASC ($r = .81$, $P < .01$), and PSC ($r = .84$, $P < .01$) contents. The ISC content of the tendon showed a direct correlation with the maximum load ($r = .85$, $P < .01$).

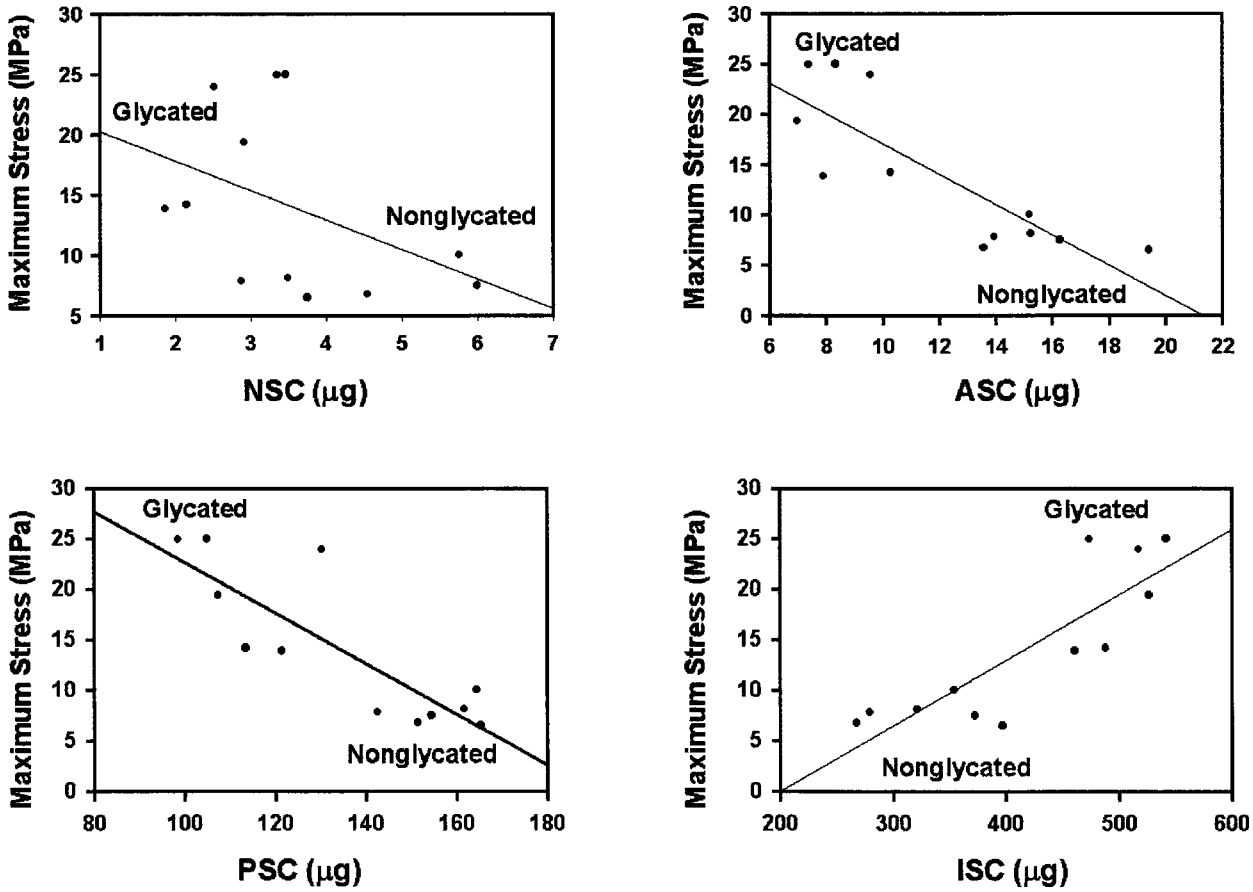

FIGURE 3

Scatterplots illustrating the correlation between the maximum stress and soluble and insoluble collagen contents from glycated and nonglycated tendons. Regression analysis showed that the maximum stress of the tendons inversely correlated with the NSC ($r = .43$, $P < .01$), ASC ($r = .83$, $P < .01$), and PSC ($r = .84$, $P < .01$) contents. The ISC content of the tendon showed a direct correlation with the maximum stress ($r = .85$, $P < .01$).

the biomechanical properties indicated that the maximum load withstood by the tendons was significantly higher in the glycated group compared to nonglycated group (50%, $P < .01$). Similarly, the maximum stress was significantly increased in glycated tendons compared to nonglycated tendons (114%, $P < .01$). However, the effect of glycation was found to be insignificant for maximum strain of the tendons (15%, $P > .05$). Young's modulus of elasticity for nonglycated tendons was significantly higher compared to glycated tendons (161%, $P < .01$).

The results in relation to energy absorption, i.e., energy to yield point, and toughness indicates that the absorption of energy in both elastic and plastic regions is significantly increased in glycated tendons compared to nonglycated tendons. This was evidenced by significant increases in energy to yield point (164%, $P < .01$) and toughness (176%, $P < .01$) in glycated tendons compared to nonglycated tendons.

The data presented above summarize the differences in the biomechanical integrity between glycated and nonglycated Achilles tendons at the maximum load point. The data collected at break point are summarized in Table 2. Significant differences were documented between the nonglycated and glycated tendons when measured for load at break and strain at break ($P < .05$). However, there were no statistically significant differences documented in other biomechanical characteristics, such as strain at break and energy absorption at break point, between the nonglycated and glycated Achilles tendons.

Biochemical Measurements

The findings of the degree of collagen cross-linking, i.e., changes in NSC, ASC, PSC, ISC, and pentosidine contents, for the tendons are presented in Table 3. The findings showed that the solubility of the NSC from glycated tendons was reduced to 61% of the nonglycated tendons, suggesting that glycation-induced cross-links may be responsible for the reduction in NSC content ($P < .01$). Similarly, ASC and PSC of the tendons were

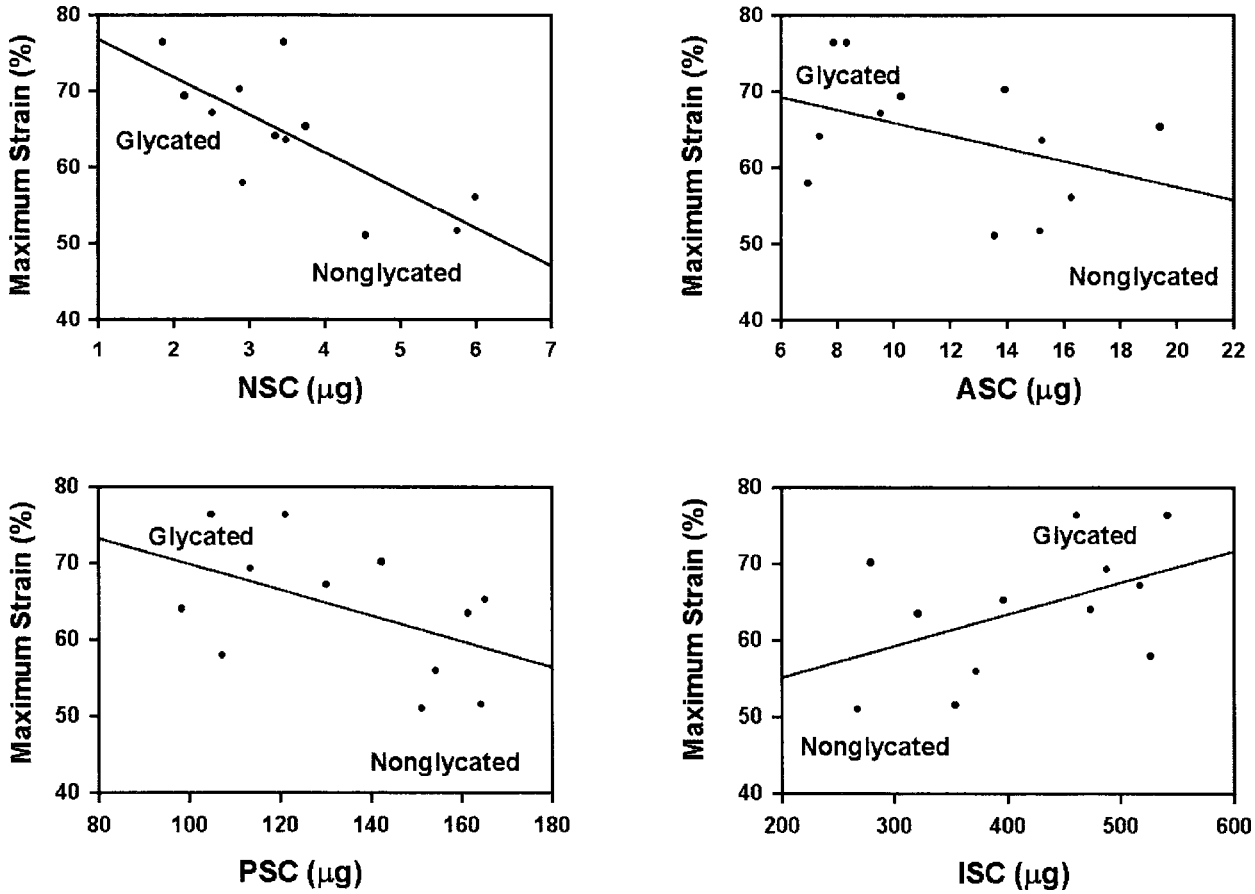

FIGURE 4
Scatterplots illustrating the correlation between the maximum strain and soluble and insoluble collagen contents from glycated and nonglycated tendons. Regression analysis showed that the maximum strain of the tendons inversely correlated with the NSC ($r = .75$, $P < .01$), ASC ($r = .40$, $P < .05$), and PSC ($r = .49$, $P < .01$) contents. The ISC content of the tendon showed a direct correlation with the maximum strain ($r = .79$, $P < .01$).

reduced to 48% and 28%, respectively, following glycation, indicating that the glycation process enhanced the resistance of tendons to acetate and pepsin treatments ($P < .01$). The amount of insoluble collagen was increased by 28% in glycated tendons compared to nonglycated tendons ($P < .01$). Furthermore, the formation of pentosidine was significantly increased in glycated tendons compared to nonglycated tendons (168%, $P < .01$).

The relative amounts of the distribution of soluble collagens in relation to total tissue collagen are shown in Figure 1. Approximately 0.5% and 0.8% of collagen was extractable in the neutral salt soluble fraction from glycated and nonglycated tendons, respectively. Using 0.5 M acetate buffer, 1.5% and 2.9% of collagen were extracted from glycated and nonglycated tendons, respectively. The results of pepsin-digested samples showed that a large amount of collagen was solubilized in both groups of tendons (20.5% for glycated tendons and 33.7% for nonglycated tendons). The percent of insoluble collagen was appreciably higher in glycated tendons (77.5%) than in nonglycated tendons (62.6%).

Relationship Between Biomechanics and Biochemistry of Collagen

Figures 2 to 7 show the relationship between biomechanical and biochemical properties for glycated and nonglycated tendons. It is interesting to note that glycation-induced collagen cross-linking is strongly associated with the alterations of the matrix biomechanics in the tendon. The results clearly demonstrate that the maximum load of the glycated tendons exhibited a significant inverse correlation with the NSC ($r = .47$, $P < .01$), ASC ($r = .81$, $P < .01$), and PSC ($r = .84$, $P < .01$) contents of the tendons. Similarly, maximum stress of glycated tendons showed a negative relationship with the levels of NSC ($r = .43$, $P < .01$), ASC ($r = .83$, $P < .01$), and PSC ($r = .84$, $P < .01$). Maximum strain displayed

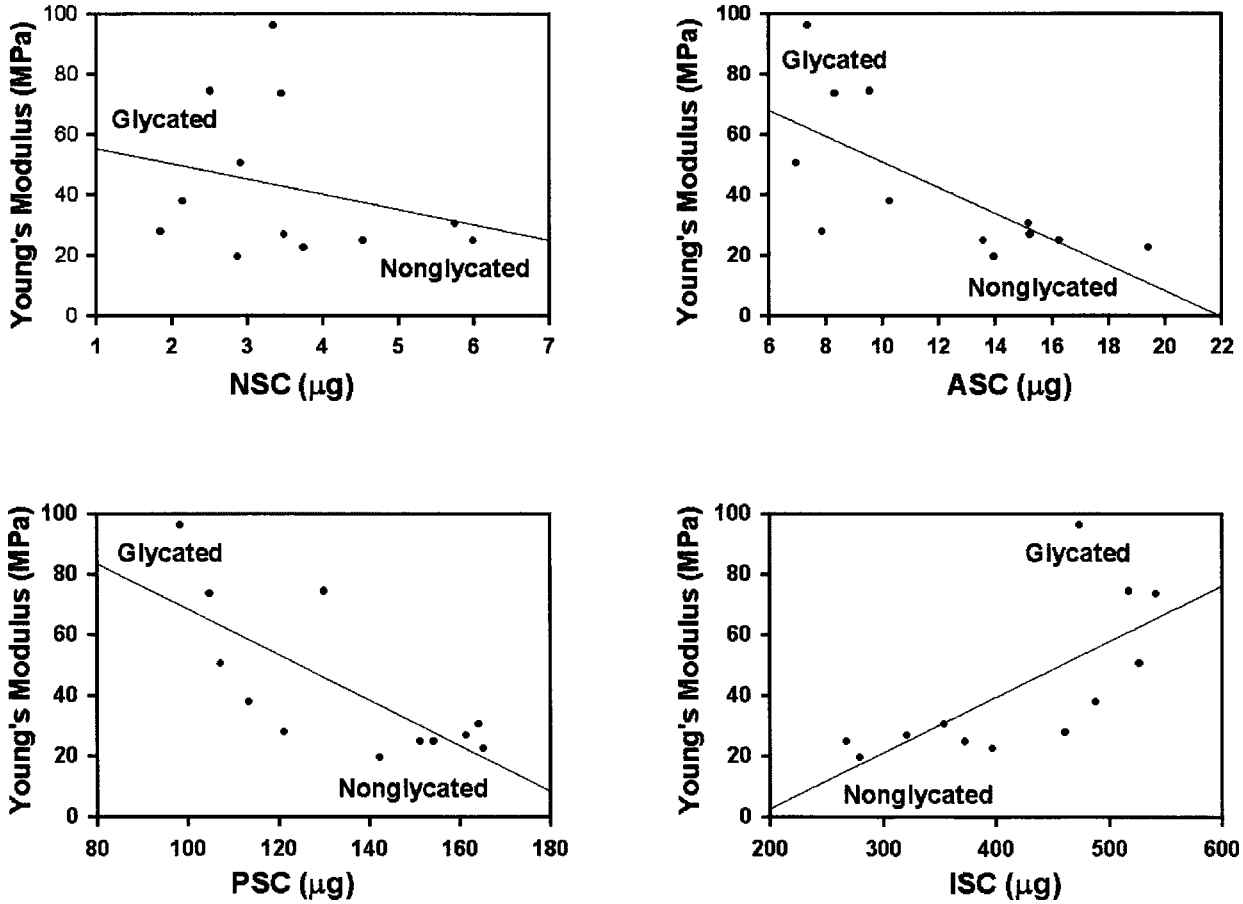

FIGURE 5
Scatterplots illustrating the correlation between the Young's modulus of elasticity and soluble and insoluble collagen contents from glycated and nonglycated tendons. Regression analysis showed that the Young's modulus of elasticity of the tendons inversely correlated with the NSC ($r = .22$, $P > .05$), ASC ($r = .65$, $P < .01$), and PSC ($r = .71$, $P < .01$) contents. The ISC content of the tendon showed a direct correlation with the Young's modulus of elasticity ($r = .61$, $P < .01$).

relatively a weak correlation with the ASC ($r = .40$, $P < .05$), PSC ($r = .49$, $P < .01$), and ISC ($r = .48$, $P > .05$) levels while exhibiting a strong inverse correlation with the NSC ($r = .75$, $P < .01$) content in glycated tendons. An inverse correlation was observed between the levels of NSC ($r = .22$, $P > .05$), ASC ($r = .65$, $P < .01$), and PSC ($r = .71$, $P < .01$) and Young's modulus of elasticity of the tendons. Similarly, the toughness of glycated tendons displayed a negative correlation with the NSC ($r = .49$, $P < .01$), ASC ($r = .77$, $P < .01$), and PSC ($r = .79$, $P < .01$) levels. However, the levels of insoluble collagen from glycated tendons showed a strong positive correlation with the maximum load (Figures 2 to 6; $r = .85$, $P < .01$), stress ($r = .85$, $P < .01$), strain ($r = .79$, $P < .01$), Young's modulus of elasticity ($r = .61$, $P < .01$), and toughness ($r = .89$, $P < .01$). The results presented in Figure 7 depict the relationship between the levels of pentosidine and various biomechanical attributes of the tendons. The pentosidine content correlated significantly with the maximum load ($r = .94$, $P < .01$), stress ($r = .92$, $P < .01$), and strain ($r = .76$, $P < .01$), Young's modulus of elasticity ($r = .75$, $P < .01$), toughness ($r = .94$, $P < .01$), and energy at break point ($r = .76$, $P < .01$). The impact of glycation showed a strong association between pentosidine and biomechanical attributes of the tendons.

DISCUSSION

Nonenzymatic glycation of the tissue proteins and subsequent production of AGEs have been implicated in the process of normal aging as well as in the pathogenesis of several diseases, including diabetes [1, 3], atherosclerosis [8], fibromyalgia [9], uremia [10, 11], Alzheimer's disease [12, 13], and renal failure [14]. Compared to other tissues, connective tissue appears to be highly vulnerable to glycation in the body. Collagen, the main organic constituent of connective tissue matrix, and

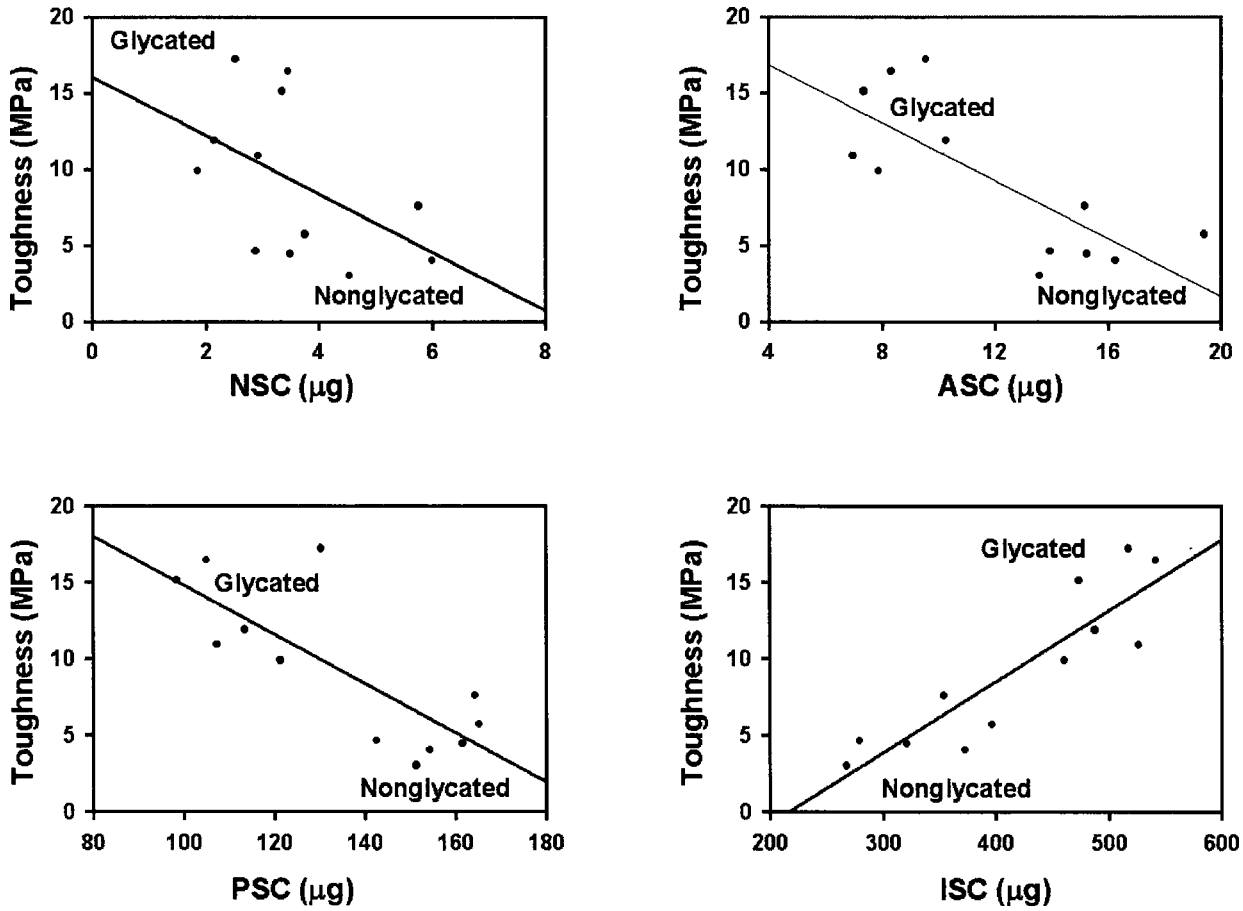

FIGURE 6
Scatterplots illustrating the correlation between the toughness and soluble and insoluble collagen contents from glycated and nonglycated tendons. Regression analysis showed that the toughness of the tendons inversely correlated with the NSC ($r = .49$, $P < .01$), ASC ($r = .77$, $P < .01$), and PSC ($r = .79$, $P < .01$) contents. The ISC content of the tendon showed a direct correlation with the toughness ($r = .89$, $P < .01$).

one of the major targets for nonenzymatic glycation, plays an important role in determining the functional properties of the tissue. Clinical complications associated with diabetes may result in functional impairment of the collagen-rich tissues, such as tendon, ligament, bone, skin, and the tunica adventitia of blood vessels, due to glycation. Recently, we have demonstrated that in vitro glycation increased the matrix stability of Achilles tendon. This study investigated not only the glycation-induced changes in the matrix stability of tissue but also the potential associations between the biomechanical attributes and biochemical properties of collagen in the tendon following an in vitro nonenzymatic glycation.

The biomechanical testing showed a significant increase in maximum load and stress, Young's modulus of elasticity, and toughness in glycated tendons compared to nonglycated tendons. The changes in the biomechanical properties of Achilles tendons by the process of nonenzymatic glycation are consistent with the previous findings reported by the author and colleagues [23] and other investigators [22, 29–31]. During biomechanical testing, the coiled or crimped collagen fibrils in the tendon are expected to align along the axis of loading. The tensile stress-strain response in tendon, in the physiological loading, is primarily due to the reorientation of bundles of fibers in the hydrated matrix [32]. The biomechanical integrity of tendon, therefore, has commonly been associated with the supramolecular organization and physical properties of the collagen fiber network.

The supramolecular organization of collagen in tendons and other tissues is primarily dependent on the degree of cross-linking. Nonenzymatic glycation is known to influence the cross-linking of collagen, and thus affect the biomechanical integrity of the tissue. In order to examine the influence of glycation on collagen cross-linking, the solubility of collagen was measured following sequential treatments with neutral and

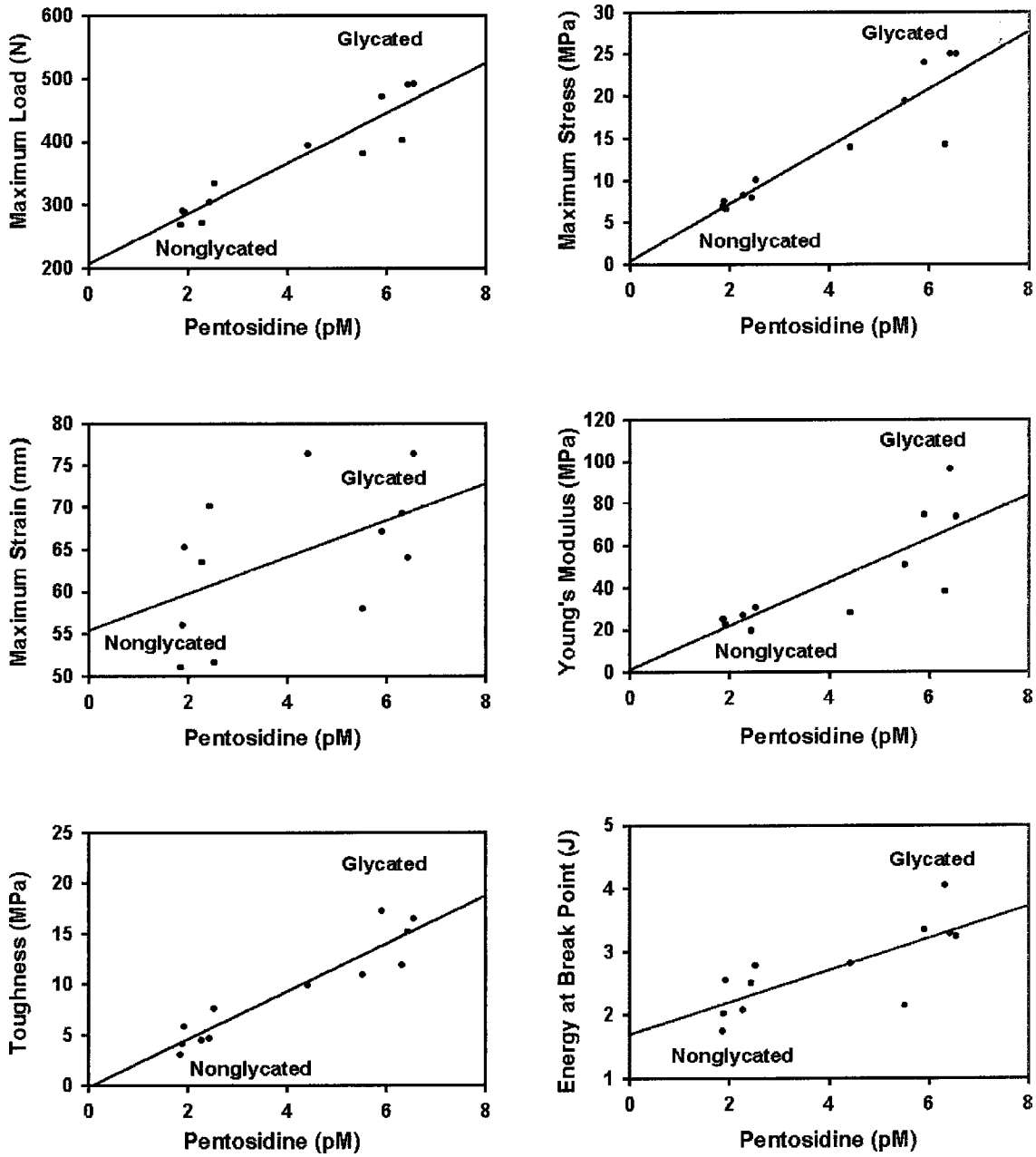

FIGURE 7

Scatterplots illustrating the correlation between the pentosidine and various biomechanical attributes of the glycated and nonglycated tendons. Regression analysis showed that the pentosidine content is directly associated with the maximum load ($r = .94$, $P < .01$), stress ($r = .92$, $P < .01$), strain ($r = .76$, $P < .01$), Young's modulus of elasticity ($r = .75$, $P < .01$), toughness ($r = .94$, $P < .01$), and energy at break point ($r = 0.76$, $P < .01$).

acetate buffer as well as with acetate buffer containing pepsin. The results of this study clearly demonstrate that the proportion of soluble collagen (in neutral buffer, weak acid, and pepsin digestible) was significantly lower in glycated tendon compared to nonglycated tendon.

The solubility of collagen in weak acid depends primarily on the extent of disruption of noncovalent and covalent bonds, but not stabilized aldimine cross-links [33]. Furthermore, collagen that is solubilized in weak acid contains more cross-links than salt-soluble collagen [34]. In this study, we observed a decrease in the proportions of acid-soluble collagen in glycated tendons compared to nonglycated tendons. Thus, the decrease in acid-soluble collagen content reflects the manifestations in acid-labile cross-links in collagen by the nonenzymatic process.

In addition, collagen in glycated tendons was highly resistive to pepsin digestion compared to nonglycated tendons. The nonhelical regions of the collagen molecules possess inter- and intramolecular cross-links [34, 35], and are the major sites for the cleavage by the proteolytic enzyme pepsin. Furthermore, the results of the collagen solubility assay demonstrate that insoluble collagen content of glycated tendons was increased significantly compared to nonglycated tendons, exhibiting marked differences in the susceptibility of collagen to proteolytic degradation.

It was our working hypothesis that the glycation-induced collagen modifications exhibit a high degree of correlation with the matrix stiffness of the tendons. This was found to be the case in that the degree of collagen cross-linking by nonenzymatic glycation showed a significant correlation with the biomechanical attributes of the tendons. The soluble collagens, such as NSC, ASC, and PSC, showed a significant inverse correlation with maximum load, stress, and strain, Young's modulus of elasticity, and toughness of the tendons. Insoluble collagen and pentosidine levels showed a strong positive correlation with the various biomechanical indices, including Young's modulus and toughness of the tendons. Young's modulus of elasticity, a direct marker of stiffness, showed a direct association with glycation cross-links, such as pentosidine, and insoluble collagen levels of the tendons. The toughness parameter that measures the energy absorption capacity of the tissue showed a direct correlation with the pentosidine and insoluble collagen levels of the tendons. Thus, the results of this study clearly demonstrate that the stiffness of the tissue directly correlated with insoluble collagen and pentosidine levels and indirectly correlated with NSC, ASC, and PSC levels of the glycated tendons.

There are several limitations to the present study. First, the results may be model or method specific. We used ribose for our in vitro study instead of glucose, which mimics to a greater extent the in vivo process of glycation during hyperglycemia and diabetes. Secondly, measurement of biomechanics revealed considerable variability in tissue stiffness. Moreover, the number of specimens was limited to 6 in each group. Due to the small sizes of the samples, such variability in the data causes difficulty with statistical analysis.

Based on our in vitro results, we conclude that glycation-induced cross-linking in collagen results in increased matrix stiffness as evaluated by measuring maximum load, stress, and strain, Young's modulus of elasticity, and toughness of the tendons. Although the levels of glycation-induced collagen cross-linking by in vivo process differs from this in vitro study, the accumulation of these collagen cross-links seems a plausible mechanism to explain the observed matrix stiffness in Achilles tendon.

REFERENCES

[1] Monnier, V. M. (1989) Toward a Maillard reaction theory of aging. *Prog. Clin. Biol. Res.,* **304,** 1–22.

[2] Brownlee, M., Cerami, A., and Vlassara, H. (1988) Advanced glycosylation end products in tissue and the biochemical basis of diabetic complications. *N. Engl. J. Med.,* **318,** 1315–1321.

[3] Brownlee, M. (1995) Advanced protein glycosylation in diabetes and aging. *Annu. Rev. Med.,* **46,** 223–234.

[4] Brownlee, M., Vlassara, H., and Cerami, A. (1984) Nonenzymatic glycosylation and the pathogenesis of diabetic complications. *Ann. Intern. Med.,* **101,** 527–537.

[5] Schnider, S. L., and Kohn, R. R. (1981) Effects of age and diabetes mellitus on the solubility and nonenzymatic glucosylation of human skin collagen. *J. Clin. Invest.,* **67,** 1630–1635.

[6] Baynes, J. W., and Thorpe, S. R. (1999) Role of oxidative stress in diabetic complications: A new perspective on an old paradigm. *Diabetes.,* **48,** 1–9.

[7] Baynes, J. W. (2001) The role of AGEs in aging: Causation or correlation. *Exp. Gerontol.,* **36,** 1527–1537.

[8] Vlassara, H. (1996) Advanced glycation end-products and atherosclerosis. *Ann. Med.,* **28,** 419–426.

[9] Hein, G., and Franke, S. (2002) Are advanced glycation end-product-modified proteins of pathogenetic importance in fibromyalgia? *Rheumatology (Oxford),* **41,** 1163–1167.

[10] Schwedler, S., Schinzel, R., Vaith, P., and Wanner, C. (2001) Inflammation and advanced glycation end products in uremia: simple coexistence, potentiation or causal relationship? *Kidney Int. Suppl.,* **78,** S32–S36.

[11] Zoccali, C., Mallamaci, F., and Tripepi, G. (2000) AGEs and carbonyl stress: Potential pathogenetic factors of long-term uraemic complications. *Nephrol. Dial. Transplant.,* **15,** 7–11.

[12] Munch, G., Schinzel, R., Loske, C., Wong, A., Durany, N., Li, J. J., Vlassara, H., Smith, M. A., Perry, G., and Riederer, P. (1998) Alzheimer's disease—synergistic effects of glucose deficit, oxidative stress and advanced glycation endproducts. *J. Neural. Transm.,* **105,** 439–461.

[13] Colaco, C. A., Ledesma, M. D., Harrington, C. R., and Avila, J. (1996) The role of the Maillard reaction in other pathologies: Alzheimer's disease. *Nephrol. Dial. Transplant.,* **11,** 7–12.

[14] Vlassara, H. (1996) Protein glycation in the kidney: Role in diabetes and aging. *Kidney Int.,* **49,** 1795–1804.

[15] Brownlee, M. (1994) Lilly Lecture 1993. Glycation and diabetic complications. *Diabetes,* **43,** 836–841.

[16] Vlassara, H., Bucala, R., and Striker, L. (1994) Pathogenic effects of advanced glycosylation: biochemical, biologic, and clinical implications for diabetes and aging. *Lab. Invest.,* **70,** 138–151.

[17] Greenwald, D. P., Shumway, S., Zachary, L. S., LaBarbera, M., Albear, P., Temaner, M., and Gottlieb, L. J. (1993) Endogenous versus toxin-induced diabetes in rats: A mechanical comparison of two skin wound-healing models. *Plast. Reconstr. Surg.,* **91,** 1087–1093.

[18] Einhorn, T. A., Boskey, A. L., Gundberg, C. M., Vigorita, V. J., Devlin, V. J., and Beyer, M. M. (1988) The mineral and mechanical properties of bone in chronic experimental diabetes. *J. Orthop. Res.,* **6,** 317–333.

[19] Menzel, E. J., and Reihsner, R. (1991) Alterations of biochemical and biomechanical properties of rat tail tendons caused by

non-enzymatic glycation and their inhibition by dibasic amino acids arginine and lysine. *Diabetologia.,* **34,** 12–16.

[20] Reiser, K. M. (1998) Nonenzymatic glycation of collagen in aging and diabetes. *Proc. Soc. Exp. Biol. Med.,* **218,** 23–37.

[21] Bellmunt, M. J., Portero, M., Pamplona. R., Cosso, L., Odetti, P., and Prat. J. (1995) Evidence for the Maillard reaction in rat lung collagen and its relationship with solubility and age. *Biochim. Biophys. Acta.,* **1272,** 53–60.

[22] Bai, P., Phua, K., Hardt, T., Cernadas, M., and Brodsky, B. (1992) Glycation alters collagen fibril organization. *Connect. Tissue. Res.,* **28,** 1–12.

[23] Reddy, G. K., Stehno-Bittel, L., and Enwemeka, C. S. (2002) Glycation-induced matrix stability in the rabbit Achilles tendon. *Arch. Biochem. Biophys.,* **399,** 174–180.

[24] Reddy, G. K., Stehno-Bittel, L., and Enwemeka, C. S. (1999) Matrix remodeling in healing rabbit Achilles tendon. *Wound. Repair. Regen.,* **7,** 518–527.

[25] Reddy, G. K., Stehno-Bittel, L., and Enwemeka, C. S. (1998) Laser photostimulation of collagen production in healing rabbit Achilles tendons. *Lasers. Surg. Med.,* **22,** 281–287.

[26] Reddy, G. K., Gum, S., Stehno-Bittel, L., and Enwemeka, C. S. (1998) Biochemistry and biomechanics of healing tendon: Part II. Effects of combined laser therapy and electrical stimulation. *Med. Sci. Sports. Exerc.,* **30,** 794–800.

[27] Reddy, G. K., and Enwemeka, C. S. (1996) A simplified method for the analysis of hydroxyproline in biological tissues. *Clin. Biochem.,* **29,** 225–229.

[28] Sell, D. R., and Monnier, V. M. (1989) Structure elucidation of a senescence cross-link from human extracellular matrix. Implication of pentoses in the aging process. *J. Biol. Chem.,* **264,** 21597–21602.

[29] Andreassen, T. T., Oxlund, H., and Danielsen, C. C. (1988) The influence of non-enzymatic glycosylation and formation of fluorescent reaction products on the mechanical properties of rat tail tendons. *Connect. Tissue. Res.,* **17,** 1–9.

[30] Andreassen, T. T., Seyer-Hansen, K., and Bailey, A. J. (1981) Thermal stability, mechanical properties and reducible cross-links of rat tail tendon in experimental diabetes. *Biochim. Biophys. Acta.,* **677,** 313–317.

[31] Galeski, A., Kastelic, J., Baer, E., and Kohn, R. .R (1977) Mechanical and structural changes in rat tail tendon induced by alloxan diabetes and aging. *J. Biomech.,* **10,** 775–782.

[32] Minns, R. J., Soden, P. D., and Jackson, D. S. (1973) The role of the fibrous components and ground substance in the mechanical properties of biological tissues: A preliminary investigation. *J. Biomech.,* **6,** 153–165.

[33] Weiss, J. B. (1976) Enzymic degradation of collagen. *Int. Rev. Connect. Tissue. Res.,* **7,** 101–157.

[34] Bornstein, P., and Traub, W. (1979) The chemistry and biology of collagen. In: *The Proteins,* Edited by Neurath, H., and Hill, R. L.), Vol. 4, pp. 411–632. New York, Academic Press.

[35] Schnider, S. L., and Kohn, R. R. (1982) Effects of age and diabetes mellitus on the solubility of collagen from human skin, tracheal cartilage and dura mater. *Exp. Gerontol.,* **17,** 185–194.

Mechanical properties and collagen cross-linking of the patellar tendon in old and young men

C. Couppé, P. Hansen, M. Kongsgaard, V. Kovanen, C. Suetta, P. Aagaard, M. Kjær and S. P. Magnusson

J Appl Physiol 107:880-886, 2009. First published 25 June 2009; doi:10.1152/japplphysiol.00291.2009

You might find this additional info useful...

This article cites 90 articles, 17 of which can be accessed free at:
/content/107/3/880.full.html#ref-list-1

This article has been cited by 29 other HighWire hosted articles, the first 5 are:

Ultrasound-based testing of tendon mechanical properties: a critical evaluation
O. R. Seynnes, J. Bojsen-Møller, K. Albracht, A Arndt, N. J. Cronin, T. Finni and S. P. Magnusson
J Appl Physiol, January 15, 2015; 118 (2): 133-141.
[Abstract] [Full Text] [PDF]

Low tendon stiffness and abnormal ultrastructure distinguish classic Ehlers-Danlos syndrome from benign joint hypermobility syndrome in patients
Rie Harboe Nielsen, Christian Couppé, Jacob Kildevang Jensen, Morten Raun Olsen, Katja Maria Heinemeier, Fransiska Malfait, Sofie Symoens, Anne De Paepe, Peter Schjerling, Stig Peter Magnusson, Lars Remvig and Michael Kjaer
FASEB J, November , 2014; 28 (11): 4668-4676.
[Abstract] [Full Text] [PDF]

Systemic stiffening of mouse tail tendon is related to dietary advanced glycation end products but not high-fat diet or cholesterol
C. Eriksen, R. B. Svensson, J. Scheijen, A. M. F. Hag, C. Schalkwijk, S. F. E. Praet, P. Schjerling, M. Kjær, S. P. Magnusson and C. Couppé
J Appl Physiol, October 15, 2014; 117 (8): 840-847.
[Abstract] [Full Text] [PDF]

The Effects of Fitness on the Aging Process
Bryan G. Vopat, Stephen A. Klinge, Philip K. McClure and Paul D. Fadale
J Am Acad Orthop Surg 2014; 22 (9): 576-585.
[Abstract] [Full Text] [PDF]

Intrinsic stiffness of extracellular matrix increases with age in skeletal muscles of mice
Lauren K. Wood, Erdan Kayupov, Jonathan P. Gumucio, Christopher L. Mendias, Dennis R. Claflin and Susan V. Brooks
J Appl Physiol, August 15, 2014; 117 (4): 363-369.
[Abstract] [Full Text] [PDF]

Updated information and services including high resolution figures, can be found at:
/content/107/3/880.full.html

Additional material and information about ***Journal of Applied Physiology*** can be found at:
http://www.the-aps.org/publications/jappl

This information is current as of April 7, 2015.

Journal of Applied Physiology publishes original papers that deal with diverse areas of research in applied physiology, especially those papers emphasizing adaptive and integrative mechanisms. It is published 12 times a year (monthly) by the American Physiological Society, 9650 Rockville Pike, Bethesda MD 20814-3991. Copyright © 2009 by the American Physiological Society. ISSN: 0363-6143, ESSN: 1522-1563. Visit our website at http://www.the-aps.org/.

Downloaded from on April 7, 2015

J Appl Physiol 107: 880–886, 2009.
First published June 25, 2009; doi:10.1152/japplphysiol.00291.2009.

Mechanical properties and collagen cross-linking of the patellar tendon in old and young men

C. Couppé,[1,2] P. Hansen,[1] M. Kongsgaard,[1] V. Kovanen,[3] C. Suetta,[1] P. Aagaard,[4] M. Kjær,[1] and S. P. Magnusson[1,2]

[1]*Institute of Sports Medicine, Bispebjerg Hospital and Center for Healthy Aging, Faculty of Health Sciences, University of Copenhagen, Copenhagen, Denmark;* [2]*Department of Physical Therapy, Bispebjerg Hospital, Copenhagen, Denmark;* [3]*Department of Health Sciences, University of Jyväskylä, Jyväskylä, Finland; and* [4]*The University of Southern Denmark, Odense, Denmark*

Submitted 1 April 2009; accepted in final form 20 June 2009

Couppé C, Hansen P, Kongsgaard M, Kovanen V, Suetta C, Aagaard P, Kjær M, Magnusson SP. Mechanical properties and collagen cross-linking of the patellar tendon in old and young men. *J Appl Physiol* 107: 880–886, 2009. First published June 25, 2009; doi:10.1152/japplphysiol.00291.2009.—Age-related loss in muscle mass and strength impairs daily life function in the elderly. However, it remains unknown whether tendon properties also deteriorate with age. Cross-linking of collagen molecules provides structural integrity to the tendon fibrils and has been shown to change with age in animals but has never been examined in humans in vivo. In this study, we examined the mechanical properties and pyridinoline and pentosidine cross-link and collagen concentrations of the patellar tendon in vivo in old (OM) and young men (YM). Seven OM (67 ± 3 years, 86 ± 10 kg) and 10 YM (27 ± 2 years, 81 ± 8 kg) with a similar physical activity level (OM 5 ± 6 h/wk, YM 5 ± 2 h/wk) were examined. MRI was used to assess whole tendon dimensions. Tendon mechanical properties were assessed with the use of simultaneous force and ultrasonographic measurements during ramped isometric contractions. Percutaneous tendon biopsies were taken and analyzed for hydroxylysyl pyridinoline (HP), lysyl pyridinoline (LP), pentosidine, and collagen concentrations. We found no significant differences in the dimensions or mechanical properties of the tendon between OM and YM. Collagen concentrations were lower in OM than in YM (0.49 ± 0.27 vs. 0.73 ± 0.14 mg/mg dry wt; $P < 0.05$). HP concentrations were higher in OM than in YM (898 ± 172 vs. 645 ± 183 mmol/mol; $P < 0.05$). LP concentrations were higher in OM than in YM (49 ± 38 vs. 16 ± 8 mmol/mol; $P < 0.01$), and pentosidine concentrations were higher in OM than in YM (73 ± 13 vs. 11 ± 2 mmol/mol; $P < 0.01$). These cross-sectional data raise the possibility that age may not appreciably influence the dimensions or mechanical properties of the human patellar tendon in vivo. Collagen concentration was reduced, whereas both enzymatic and nonenzymatic cross-linking of concentration was elevated in OM vs. in YM, which may be a mechanism to maintain the mechanical properties of tendon with aging.

tendon dimension; tendon mechanical properties; aging; collagen; hydroxylysyl pyridinoline; lysyl pyridinoline; advanced glycation end products

FORCE GENERATED BY MUSCLE is transferred to bones via tendons to produce movement. However, tendons are not entirely inextensible, but exhibit elastic and time-dependant properties that serve to influence the overall function of the muscle-tendon complex (3, 13, 17, 29, 58). Tendons have traditionally been considered relatively inert structures, but several recent reports have demonstrated that human tendons respond directly to physical activity by increased metabolic activity (15, 35, 42) and increased collagen synthesis (50, 51). Furthermore, strength training and habitual loading of tendons appear to be associated with increased tendon size (6, 21, 46), confirming that the aforementioned response to elevated loading results in a net increase of tendon tissue. These recent findings show that tendons respond and adapt to their specific loading history.

Aging is associated with a decline in muscle mass, strength, and physical function (66). However, although tendon properties influence the overall function of the muscle-tendon complex (58, 67), there is a relative lack of human data that describe possible age-associated changes in mechanical properties of tendon. Animal data show that aging yields a stronger and stiffer tendon (34, 69, 83), a weaker and more compliant tendon (27, 90, 91), or leaves the tendon unchanged (39); thus these data are inconclusive. In contrast, data on isolated human cadaver tendon suggest that the aging process largely leaves the mechanical properties unaltered (31, 40, 41). Despite the development of ultrasonography-based methods to evaluate human tendon properties in vivo (33, 37, 53), the effect of aging on the mechanical properties of human tendon in vivo remains elusive. Tendon strain in humans has been shown to decrease (47–49) or increase (43, 52, 61, 63, 70) with aging. Yet others have shown that aging leaves the mechanical properties of the patellar tendon unchanged (18). Thus the picture is incoherent, which may partly be related to methodological and design differences, the physical activity level of the sample population, and the type of tendon tested, i.e., the tendon-aponeurosis complex or the free tendon alone.

In tendon, the trivalent intermolecular pyridinoline cross-links [primarily hydroxylysyl pyridinoline (HP) and lysyl pyridinoline (LP)] stabilize the fibrillar structure of collagen and thus contribute to the mechanical properties of the tendon (7, 9, 12). These cross-links are formed from enzymatically derived covalent immature cross-links, which undergo a spontaneous conversion into more mature trivalent cross-links with collagen maturation (7). The slow turnover of mature collagen allows further cross-linking via the adventitious nonenzymatic reactions of glucose with the lysyl and arginine amino acid residues in the collagen triple helix as a true aging process (7, 59, 62). This nonenzymatic process results in the accumulation of advanced glycation end products (AGE) in tendon tissue. The most widely studied AGE is pentosidine. AGE accumulation is known to accelerate with aging and diabetes (16, 28, 62) and is believed to yield a stiffer and more load-resistant tendon (78, 79). It has been shown that AGE cross-link density in collag-

Address for reprint requests and other correspondence: S. P. Magnusson, Institute of Sports Medicine Copenhagen, Bispebjerg Hospital, Bldg. 8, 1st Floor, Bispebjerg Bakke 23, 2400 Copenhagen NV, Denmark (e-mail: P.Magnusson@mfi.ku.dk).

 8750-7587/09 $8.00 Copyright © 2009 the American Physiological Society

Downloaded from on April 7, 2015

enous tissues (19, 38, 81, 86) and in human tendons (11, 84) is markedly higher in older than in younger individuals, and there are only sparse human data on mature cross-link density of tendon and how these are influenced by aging (11). However, recent reports of an age-associated reduction in human tendon stiffness in vivo (43, 52, 61, 63, 70) in conjunction with the notion of simultaneously elevated cross-link density and AGE accumulation are difficult to reconcile. To the best of our knowledge, there are currently no human studies examining collagen cross-linking and mechanical properties of the patellar tendon in vivo in old and young men. Therefore, the purpose of this study was to examine both the mechanical properties of human patellar tendon in vivo and collagen cross-link composition in old (OM) and young men (YM) subjects.

MATERIALS AND METHODS

Subjects. Seven OM (67 ± 3 years, 86 ± 10 kg) and 10 YM (27 ± 2 years, 81 ± 8 kg) with similar activity levels volunteered for the study (Table 1). With the use of a standardized form, participants were interviewed regarding how many hours per week they were performing organized sport or exercise on a regular basis (OM: 5 ± 6 h/wk, YM: 5 ± 2 h/wk). There were no differences in physical characteristics between OM and YM. All were healthy, did not take prescription medicine, and had no overt signs or symptoms of diabetes. In addition, the subjects had no known knee or tendon pathology. The study complied with the Declaration of Helsinki and was approved by the local ethics committee. All subjects gave their informed consent before the experiments.

Muscle and tendon dimensions. The anatomic cross-sectional area (CSA) of the quadriceps femoris muscle was measured 20 cm proximal to the tibia plateau (mid-thigh level) by magnetic resonance imaging (MRI) (General Electric, Sigma Horizon LX 1.5-Tesla, T1 weighted SE) using a lower extremity coil. The images were obtained using the following parameters: TR/TE = 500/14 ms, field of view (FOV) = 18, matrix = 512 × 512, and slice thickness = 6 mm (21, 46). Subsequently, the lean muscle mass of the quadriceps muscle (subcutaneous and intermuscular noncontractile tissues were excluded from the measurement) was manually outlined using the software program Osiris 4.19 (http://www.sim.hcuge.ch/osiris/). The mean value of three measurements of the same image was used for analysis. Patellar tendon CSA and length were determined with the use of MRI (General Electric, Sigma Horizon LX, 1.5-Tesla, T1 weighted SE) (21, 46). Patellar tendon CSA was determined by axial plane MRI using the following parameters: TR/TE = 400/14 ms, FOV = 20, matrix = 256 × 256, slice thickness = 5.0 mm, and spacing = 0 mm. The axial scans were performed perpendicular to the patellar tendon. As described in detail previously, the tendon CSA was measured *1*) just distal to the patellar insertion, *2*) just proximal to the tibia insertion, and *3*) midway between these two sites (21, 46). The patellar tendon length was determined from sagittal plane MRI using the following parameters: TR = 500, echo time (ET) = 3 × (TE: 12.4 ms), FOV = 16, matrix = 256 × 192, slice thickness = 4.0 mm, and no spacing. The patellar tendon length was obtained by measuring the distance from the dorsal insertion at the patella apex to the dorsal insertion on the tibia. Patellar tendon CSA and length were manually outlined using the software program Osiris 4.19 (http://www.sim.hcuge.ch/osiris/). The color intensity of each image was adjusted using the National Institutes of Health color scale mode of the software. Tendon CSA and length were measured using the grayscale image display. The average tendon CSA was calculated from the three levels (proximal, mid, and distal CSA) and used for analysis. The typical error percent of repeated measures of site-specific tendon CSA was 2–2.5% (21).

Table 1. *Physical characteristics of OM and YM*

	OM (n = 7)	YM (n = 10)
Age, years	67±3	27±2
Height, cm	178±9	183±4
Weight, kg	86±10	81±8
Activity level, h/wk	5±6	5±2

Values are means ± SD. There were no differences in physical characteristics between old men (OM) and young men (YM).

Mechanical properties of tendon. The details of the measurement, including the reliability of the method in our laboratory, has been reported previously (37). The within-day correlation coefficient and typical error percent results for repeated measures were 0.95 and 9.9% for tendon stiffness, 0.97 and 5.5% for tendon strain, and 0.94 and 9.4% for Young's modulus. Subjects performed a 5-min warm-up on a stationary bike to secure proper preconditioning of the tendon before testing. Thereafter, the subjects were seated in a custom-made rigid chair with both hips and knees flexed to an angle of 90°. A leg cuff, which was connected to a strain gauge (Bofors KRG-4, Bofors, Sweden) through a rigid steel rod perpendicular to the lower leg, was mounted on the leg just above the medial malleolus. An ultrasound probe (7.5 MHz, linear array B-mode; Sonoline Sienna, Siemens, Erlangen, Germany) was fitted into a custom-made rigid cast that was secured to the skin above the patellar tendon in the sagittal plane. The ultrasound probe and cast were positioned so that the patella, the patellar tendon, and the tibia were all visible within the viewing field throughout the ramped contractions (Fig. 1).

The ultrasound S-VHS video images obtained during the ramp trials were sampled at 50 Hz on a personal computer using frame-by-frame capturing software (Matrox Marvel G400-TV, Dorval, Quebec, Canada). Force was sampled on two separate personal computers at 50 Hz via a 12-bit analog-to-digital converter (dt2810A; Data Translation). The two computers were interconnected to permit synchronous sampling of all data using a custom-built trigger device (14). The subjects performed four to five slow isometric knee extensions ramps by applying gradually increasing force until maximum over a 10-s period during which patellar tendon displacement and knee extension force were measured simultaneously. Each ramp was separated by a 2-min rest period. All measurements were performed on one side, randomized to either the right or left knee. During the ramp contractions, force was sampled at 50 Hz and low-pass filtered at a 1.0-Hz cutoff frequency using a fourth-order zero-lag Butterworth filter.

Tendon force was calculated by dividing the estimated total knee extension moment by the internal moment arm, which was estimated from individually measured femur lengths (87). Tendon stress was calculated by dividing tendon force with the average of the three levels (proximal, mid, and distal) of the patellar tendon CSA determined from MRI. Tendon deformation was defined as the change in distance between the patellar apex and the tibia (37, 57). Tendon strain was calculated as the change in length related to the initial tendon length. Each single force-deformation curve was fitted to a second- or third-order polynomial fit, which yielded $R^2 > 0.98$. Tendon stiffness (Δforce/Δdeformation) and Young's modulus (Δstress/Δstrain) based on common force were calculated in the final 20% of the force-deformation and stress-strain curves, respectively (57). To compare tendon dimensions between the subjects of various body size, tendon CSA data were normalized to body weight and raised to the power of 2/3 (60).

Patellar tendon biopsies. A Bard MAGNUM biopsy instrument (C.R. Bard, Covington, GA) with a disposable core biopsy needle (14 gauge) was used. After sterilization, the skin was injected with local anesthetic (1% lidocaine), and a 3- to 5-mm-long incision was created just distal to the patella apex. The biopsy needle was inserted into the tendon surface at an ~30° angle and fired, securing a tissue sample of ~8 mg. Samples were snap-frozen in liquid nitrogen and stored at −80°C. Tendon biopsies were taken from the same side as tendon mechanical properties assessments were performed. No previous bi-

Downloaded from on April 7, 2015

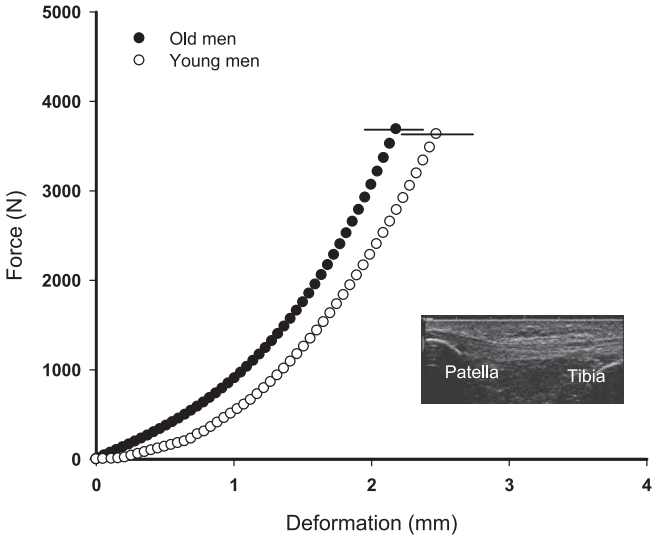

Fig. 1. The patellar tendon force-deformation relationship based on common force. Values are means ± SD of all subjects. There were no differences between old (OM) and young men (YM) with respect to tendon deformation or stiffness ($P > 0.05$).

opsy had been taken from that site in all subjects. All biopsy samples were analyzed in an investigator-blinded fashion.

Biochemical analysis. Freeze-dried tendon samples were hydrolyzed in 6 M HCl (+108 C, 24 h) and evaporated into dryness and dissolved in H_2O. Hydroxyproline, the collagen-specific amino acid, was measured spectrophotometrically (23) to quantify collagen protein (24). HP, LP, and pentosidine were analyzed via a single reversed-phase high-performance liquid chromatography (HPLC) run and detected on the basis of their natural fluorescence (10). At 0–16 min, the wavelength for HP and LP fluorescence was 400 nm for emission and 295 nm for excitation. The wavelengths were changed at 16–60 min to 328/378 nm to measure pentosidine. For the elution of the cross-links, a gradient was built up to contain 17% eluent B (75% acetonitrile with 0.13% heptafluorobutyric anhydride) at 0 min and 25% eluent B at 30 min. Eluent A was 0.13% heptafluorobutyric anhydride. Flow rate was 1 ml/min. HP was eluted at 12 min, LP at 13.5 min, and pentosidine at 23 min. The HPLC system used included Quaternary Gradient Pump unit, PU-2089 Plus, Intelligent AutosamplerAS-2057 Plus, and Intelligent Fluorescence Detector FP-2020 by Jasco. Data processing software was Jasco Chrompass. The LiChroCART 125-4 column was from Merck Hitachi. The results for HP, LP, and pentosidine are given compared with the standards injected at four different concentrations in each HPLC run. The intra-assay coefficient of variations based on duplicates within a run were 2.6%, 3.7%, and 3.9% for HP, LP, and pentosidine, respectively. The detection limit for HP and LP is 0.4 pmol and 0.05 pmol for pentosidine.

Data reduction and analysis. The two isometric ramp contractions that yielded the greatest maximum force were selected for further analysis. To make group comparisons and thereby account for differences in magnitude in isometric ramp contraction force, the trials for all subjects were subsequently analyzed to the lowest common force, as determined by the weakest subject (3953 N). Mann-Whitney *U*-tests were used to examine whether there were differences between the groups in the measured variables. Spearman rank-order correlation was used to analyze the strength of relationships between variables. $P < 0.05$ was considered significant. Results are reported as means ± SD.

RESULTS

Peak knee extensor moment was lower in OM (154 ± 41 N·m) than in YM (216 ± 62 N·m) ($P < 0.05$). Similarly, quadriceps femoris CSA was lower in OM than in YM (Table 2) ($P < 0.01$).

Table 2. *Patellar tendon dimensions and quadriceps muscle CSA for OM and YM*

	OM (n = 7)	YM (n = 10)
Tendon length, mm	43±4	43±5
Tendon CSA, mm^2	101±17	103±8
Tendon CSA, mm^2/body $wt^{2/3}$	5.34±0.48	5.47±0.25
Quadriceps muscle CSA, mm^2	6,214±705*	8,431±522

Values are means ± SD. CSA, cross-sectional area. *Significantly different from YM, $P < 0.01$.

Tendon dimensions are shown in Table 2. Tendon length did not differ between YM and OM. Absolute average tendon CSA did not differ between OM and YM. Similarly, there was no between group difference in average tendon CSA normalized for body weight.

Mechanical properties determined at maximal force are shown in Table 3. Maximal tendon force was lower in OM than in YM ($P < 0.05$). There were no differences between OM and YM with respect to tendon deformation, stiffness, strain, stress, or Young's modulus based on average tendon CSA. Mechanical properties at a common force are shown in Table 4. Again, there were no differences between OM and YM for any of the variables (Figs. 1 and 2).

Collagen concentration and cross-link density data are shown in Table 5. Collagen concentration was lower in OM than in YM ($P < 0.05$). Both HP and LP ($P < 0.05$) as well as pentosidine ($P < 0.01$) concentrations in collagen were higher in OM than in YM. Pentosidine was positively related to age in YM ($r = 0.74$, $P < 0.01$, Fig. 3) but not in OM ($r = 0.65$, $P = 0.11$). There were no significant correlations between the mechanical and biochemical variables.

DISCUSSION

To the best of our knowledge, this is the first study that has examined both the mechanical properties of the human patellar tendon in vivo and collagen cross-link densities in YM and OM with similar physical activity levels. The main findings were that the collagen concentration was lower in OM than in YM, whereas the enzymatically derived cross-links (HP and LP) were greater in OM than in YM. At the same time, the nonenzymatically derived AGE marker (pentosidine) was markedly more abundant in OM than in YM. However, despite these apparent age-related differences in the tendon collagen properties, the tendon mechanical properties in the two age groups did not diverge appreciably.

It is well known that age is associated with a loss in muscle mass and consequently a reduction in muscle function (66). It

Table 3. *Patellar tendon mechanical properties for OM and YM based on maximum force*

	OM (n = 7)	YM (n = 10)
Force, N	5,161±737*	7,415±2184
Deformation, mm	2.6±0.4	2.9±0.9
Stiffness, N/mm	3,926±1091	5,546±1871
Stress, MPa	51±8	65±24
Strain, %	6.1±0.9	6.9±2.3
Modulus, GPa	1.7±0.3	2.2±0.7

Values are means ± SD. *Significantly different from YM, $P < 0.05$.

Downloaded from on April 7, 2015

Table 4. *Patellar tendon mechanical properties for OM and YM based on common force*

	OM (n = 7)	YM (n = 10)
Deformation, mm	2.3±0.4	2.4±0.6
Stiffness, N/mm	3,511±837	3,290±869
Stress, MPa	41±7	37±5
Strain, %	5.3±0.9	5.9±1.7
Modulus, GPa	1.5±0.4	1.4±0.4

Values are means ± SD.

Table 5. *Concentration of collagen and hydroxylysyl pyridinoline, lysyl pyridinoline, and pentosidine cross-links in the patellar tendons of OM and YM*

	OM (n = 7)	YM (n = 10)
Collagen, mg/mg dry wt	0.49±0.27*	0.73±0.14
Hydroxylysyl pyridinoline, mmol/mol collagen	898±172*	645±183
Lysyl pyridinoline, mmol/mol collagen	49±38†	16±8
Pentosidine, mmol/mol collagen	73±13†	11±2

Values are means ± SD. *,†Significantly different from the values of YM ($P < 0.05$ and $P < 0.01$, respectively).

has also been suggested that tendon compliance and electromechanical delay increase with aging (80), which would reduce efficient transfer of contractile force and therefore amplify the age-associated decline in muscle function. However, to what extent the mechanical properties of human tendon change with aging remains unclear. Data based on animal models are disjointed as they suggest that aging reduces (27, 90, 91), augments (34, 69, 83), or leaves the mechanical properties unchanged (39). Similarly, data based on human in vivo models are inconclusive. These studies show that, with aging, the tendon becomes more compliant (43, 52, 61, 63, 70), less compliant (47–49), or remains unchanged (18, 43). In contrast, data on isolated human cadaver preparations consistently suggest that aging does not influence the mechanical properties (31, 40, 41), which is in agreement with the present data and that of Carroll et al. (18) on human patellar tendon in vivo.

The present mechanical data diverge from those of others based on the human in vivo model with one exception (18), and this may be related to methodological differences and study design. It has been shown that strength training and habitual loading pattern may result in tendon hypertrophy (6, 21, 46), which would influence the mechanical properties of the tendon (80). In contrast to previous in vivo studies (18, 43, 47, 52, 61, 63, 70), we have taken this aspect into account by comparing age groups with similar activity levels. However, it cannot be ruled out that prior life-long training history, including exercise mode and intensity, which was unaccounted for in the study, may have influenced the data. Furthermore, it has been shown that the ultrasonography-based method of obtaining patellar tendon deformation requires that the movement of the tibia also has to be considered (37, 71), which was achieved in the present study and in the study by Carroll et al. (18). Notably, the present data and that of Carroll et al. (18) cannot demonstrate any age-associated difference in mechanical properties of the patellar tendon. Moreover, several studies have investigated the effect of aging on the mechanical properties based on a composite measure of deformation that includes both that of the tendon and aponeurosis, rather than the tendon per se (43, 52, 61, 63, 70). This makes direct comparisons of results difficult since the free tendon and aponeurosis have dissimilar mechanical properties and because the stiffness of the aponeurosis can be modulated during contraction (30, 57). It should also be recognized that the present data and that of others are based on cross-sectional designs with inherent limitations, including the striking variations in tendon mechanical properties between subjects (54); therefore, a type II error cannot be ruled out.

The densities of mature lysyl oxidase-derived intermolecular covalent cross-links, such as HP and LP, gradually increase during tendon tissue maturation, and it is commonly believed that these cross-links are the chief contributors to the function and mechanical properties of the tendon (7, 9, 12, 76). In animal models, it has been shown that there is a positive

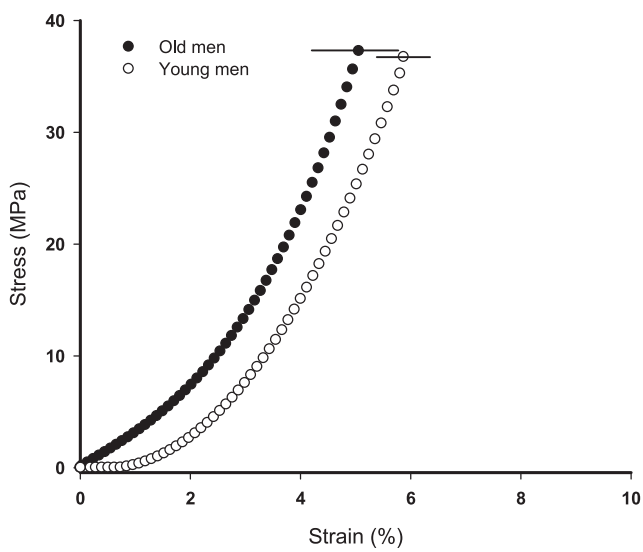

Fig. 2. The patellar tendon stress-strain relationship based on common force. Values are means ± SD of all subjects. There were no differences between OM and YM with respect to tendon strain, stress, or Young's modulus based on average tendon cross-sectional area ($P > 0.05$).

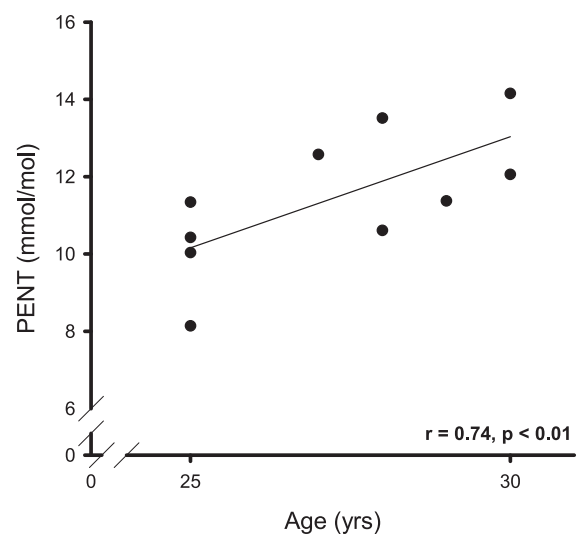

Fig. 3. Pentosidine was positively related to age in YM ($r = 0.74$, $P < 0.01$).

Downloaded from on April 7, 2015

relationship between HP cross-link density and mechanical strength of the healing medial collateral ligament tissue and anterior cruciate ligament graft (32, 68) and furthermore that changes in HP and LP density will result in altered mechanical properties in collagenous tissue (7, 72). However, there are only sparse human data on mature cross-link density in tendon and how these are influenced by aging (11). A small but significant age-related increase of LP has been demonstrated in the supraspinatus tendon in vitro (11). The present data on LP and HP densities of YM correspond well with previously reported data in a similar population (45). However, the present data also demonstrate that HP and LP densities of the human patellar tendon were ~40% and threefold higher, respectively, in OM than in YM, suggesting a rather marked age-associated elevation in these enzymatic cross-links. It is noteworthy that, despite the rather robust difference in both HP and LP, there was no difference in the mechanical properties of the tendon. However, it should be noted that fibril length (22, 77), fibril diameter (74), and proteoglycans and glycosaminoglycans (44, 73, 75) have all been implicated in contributing to the tendon mechanical properties, and the relative contribution of these factors and that of mature cross-links remains elusive.

To our knowledge, these are the first data showing that AGE is markedly increased in the human patellar tendon of OM vs. in that of YM. AGE cross-links, including pentosidine, are formed when lysine amino acid residues in the collagen triple helix come into contact with glucose (7, 62), and the accumulation of these cross-links is known to accelerate with aging (7, 44) and disease processes such as diabetes (16, 28, 62), atherosclerosis (88), Alzheimer (20, 64), and renal failure (89). AGE products are also used as markers of tissue turnover (11). It has been shown that the difference between young and older individuals in AGE cross-link density in collagen is ~2-fold in human skeletal muscle (38), 5-fold in human bone (81), 7-fold in human tendon (present data), 9-fold in human ligaments (19), and 33-fold in human cadaver cartilage (86), demonstrating the tissue-specific turnover. The fact that pentosidine density is sevenfold greater in tendon of OM than in YM (Table 5), coupled with the fact that pentosidine appears to be related to age in a narrow age span (Fig. 3), firmly demonstrates the positive relationship between AGE cross-linking of human patellar tendon collagen and aging ex vivo. These data corroborate and extend those previously reported on cadaver tissue (11, 84). From a functional standpoint, an elevated AGE cross-link density has been suggested to result in increased tensile stress and tendon stiffness in animal models (4, 5, 8, 34, 78, 79, 85). However, in the present study, both the stiffness (Fig. 1) and the Young's modulus (Fig. 2) of the tendon did not differ between OM and YM despite the sevenfold difference in pentosidine, suggesting that factors other than AGE may also play a major role in determining the mechanical properties of human tendon.

In the present study, the total collagen concentration of the patellar tendon was ~34% lower in OM than in YM (Table 5), and this age-linked reduction is in accordance with that found in the canine patellar tendon (39) and rat tail tendon (90). It is possible that the lower collagen concentration with aging may represent the reduced size and/or density of collagen fibrils that is known to occur with aging (26, 65, 74, 76, 82). It was recently reported that MRI signal intensity of the patellar tendon was reduced with aging (18), which may be a function of the reduction in collagen concentration observed in the present study. Unfortunately, the size of the obtained biopsy in the present study precluded transmission electron microscopy analysis for fibril size and density. The lower collagen concentration in OM may be an age-related change in the tendon per se and/or a function of reduced tendon loading due to an age-related loss of muscle mass/strength. Interestingly, the average whole tendon CSA did not differ between OM and YM (Table 2), which in light of the reduced collagen concentration may be related to increased amounts of other extracellular matrix components, such a proteoglycans and glycosaminoglycans. Alternatively, the retained tendon CSA in OM may result from tendon intrafibrillar fat that can accumulate with aging (1, 2, 25). It has previously been demonstrated that the Achilles tendon CSA is larger in postmenopausal women than in young women (55), but it should be noted that female hormones may significantly impact collagen synthesis (36, 56). This potential sex-dependent factor is the reason that we have undertaken the present study in men only.

Albeit speculative, it is possible that the elevated enzymatic and/or nonenzymatic cross-link density in OM vs. that shown in YM served to maintain tendon stiffness and Young's modulus despite the diminished collagen concentration. Such maintenance of tendon stiffness would serve to maintain effective transfer of muscle force despite a lower absolute muscle size (Table 2) and strength (Table 3). In this context, it should be noted that the present data were obtained in moderately physically active individuals, and future studies will need to address the effect of training per se in elderly.

In conclusion, results from the present study raise the possibility that the dimensions and mechanical properties of the human patellar tendon in vivo may not differ between OM and YM. On the other hand, the OM group displayed lower collagen concentration, but greater enzymatic (HP and LP) and nonenzymatic (pentosidine) collagen cross-links, than YM. This age-related increase in both enzymatic and nonenzymatic cross-linking compounds may serve to maintain the mechanical properties of tendon with aging.

ACKNOWLEDGMENTS

The technical assistance of Kaisa-Leena Tulla (Department of Health Sciences, University of Jyväskylä, Finland) in the HPLC analyses is greatly acknowledged.

GRANTS

This study was supported by Team Danmark Research Foundation, Center for Healthy Aging, The Danish Physiotherapy Association, and Danish Medical Research Council.

REFERENCES

1. **Adams CW, Bayliss OB.** Acid mucosubstances underlying lipid deposits in ageing tendons and atherosclerotic arteries. *Atherosclerosis* 18: 191–195, 1973.
2. **Adams CW, Bayliss OB, Baker RW, Abdulla YH, and Hunter-Craig CJ.** Lipid deposits in ageing human arteries, tendons and fascia. *Atherosclerosis* 19: 429–440, 1974.
3. **Alexander RM, Net-Clark HC.** Storage of elastic strain energy in muscle and other tissues. *Nature* 265: 114–117, 1977.
4. **Andreassen TT, Oxlund H, Danielsen CC.** The influence of nonenzymatic glycosylation and formation of fluorescent reaction products on the mechanical properties of rat tail tendons. *Connect Tissue Res* 17: 1–9, 1988.
5. **Andreassen TT, Seyer-Hansen K, Bailey AJ.** Thermal stability, mechanical properties and reducible cross-links of rat tail tendon in experimental diabetes. *Biochim Biophys Acta* 677: 313–317, 1981.

Downloaded from on April 7, 2015

6. **Arampatzis A, Karamanidis K, Albracht K.** Adaptational responses of the human Achilles tendon by modulation of the applied cyclic strain magnitude. *J Exp Biol* 210: 2743–2753, 2007.
7. **Avery NC, Bailey AJ.** Enzymic and non-enzymic cross-linking mechanisms in relation to turnover of collagen: relevance to aging and exercise. *Scand J Med Sci Sports* 15: 231–240, 2005.
8. **Bai P, Phua K, Hardt T, Cernadas M, Brodsky B.** Glycation alters collagen fibril organization. *Connect Tissue Res* 28: 1–12, 1992.
9. **Bailey AJ.** Molecular mechanisms of ageing in connective tissues. *Mech Ageing Dev* 122: 735–755, 2001.
10. **Bank RA, Beekman B, Verzijl N, de Roos JA, Sakkee AN, TeKoppele JM.** Sensitive fluorimetric quantitation of pyridinium and pentosidine crosslinks in biological samples in a single high-performance liquid chromatographic run. *J Chromatogr B Biomed Sci Appl* 703: 37–44, 1997.
11. **Bank RA, TeKoppele JM, Oostingh G, Hazleman BL, Riley GP.** Lysylhydroxylation and non-reducible crosslinking of human supraspinatus tendon collagen: changes with age and in chronic rotator cuff tendinitis. *Ann Rheum Dis* 58: 35–41, 1999.
12. **Barnard K, Light ND, Sims TJ, Bailey AJ.** Chemistry of the collagen cross-links. Origin and partial characterization of a putative mature cross-link of collagen. *Biochem J* 244: 303–309, 1987.
13. **Biewener A, Baudinette R.** In vivo muscle force and elastic energy storage during steady-speed hopping of tammar wallabies (*Macropus eugenii*). *J Exp Biol* 198: 1829–1841, 1995.
14. **Bojsen-Moller J, Hansen P, Aagaard P, Kjaer M, Magnusson SP.** Measuring mechanical properties of the vastus lateralis tendon-aponeurosis complex in vivo by ultrasound imaging. *Scand J Med Sci Sports* 13: 259–265, 2003.
15. **Bojsen-Moller J, Kalliokoski KK, Seppanen M, Kjaer M, Magnusson SP.** Low-intensity tensile loading increases intratendinous glucose uptake in the Achilles tendon. *J Appl Physiol* 101: 196–201, 2006.
16. **Brownlee M.** Advanced protein glycosylation in diabetes and aging. *Annu Rev Med* 46: 223–234, 1995.
17. **Butler DL, Grood ES, Noyes FR, Zernicke RF.** Biomechanics of ligaments and tendons. *Exerc Sport Sci Rev* 6: 125–181, 1978.
18. **Carroll CC, Dickinson JM, Haus JM, Lee GA, Hollon CJ, Aagaard P, Magnusson SP, Trappe TA.** Influence of aging on the in vivo properties of human patellar tendon. *J Appl Physiol* 105: 1907–1915, 2008.
19. **Chen JR, Takahashi M, Kushida K, Suzuki M, Suzuki K, Horiuchi K, Nagano A.** Direct detection of crosslinks of collagen and elastin in the hydrolysates of human yellow ligament using single-column high performance liquid chromatography. *Anal Biochem* 278: 99–105, 2000.
20. **Colaco CA, Ledesma MD, Harrington CR, Avila J.** The role of the Maillard reaction in other pathologies: Alzheimer's disease. *Nephrol Dial Transplant* 11, Suppl 5: 7–12, 1996.
21. **Couppe C, Kongsgaard M, Aagaard P, Hansen P, Bojsen-Moller J, Kjaer M, Magnusson SP.** Habitual loading results in tendon hypertrophy and increased stiffness of the human patellar tendon. *J Appl Physiol* 105: 805–810, 2008.
22. **Craig AS, Birtles MJ, Conway JF, Parry DA.** An estimate of the mean length of collagen fibrils in rat tail-tendon as a function of age. *Connect Tissue Res* 19: 51–62, 1989.
23. **Creemers LB, Jansen DC, van Veen-Reurings A, van den BT, Everts V.** Microassay for the assessment of low levels of hydroxyproline. *Biotechniques* 22: 656–658, 1997.
24. **Creemers LB, Jansen DC, van Veen-Reurings A, van den BT, Everts V.** Microassay for the assessment of low levels of hydroxyproline. *Biotechniques* 22: 656–658, 1997.
25. **Crouse JR, Grundy SM, Ahrens EH Jr.** Cholesterol distribution in the bulk tissues of man: variation with age. *J Clin Invest* 51: 1292–1296, 1972.
26. **Curwin SL, Roy RR, Vailas AC.** Regional and age variations in growing tendon. *J Morphol* 221: 309–320, 1994.
27. **Dressler MR, Butler DL, Wenstrup R, Awad HA, Smith F, Boivin GP.** A potential mechanism for age-related declines in patellar tendon biomechanics. *J Orthop Res* 20: 1315–1322, 2002.
28. **Dyer DG, Dunn JA, Thorpe SR, Bailie KE, Lyons TJ, McCance DR, Baynes JW.** Accumulation of Maillard reaction products in skin collagen in diabetes and aging. *J Clin Invest* 91: 2463–2469, 1993.
29. **Elliott DH.** Structure and function of mammalian tendon. *Biol Rev Camb Philos Soc* 40: 392–421, 1965.
30. **Finni T, Hodgson JA, Lai AM, Edgerton VR, Sinha S.** Nonuniform strain of human soleus aponeurosis-tendon complex during submaximal voluntary contractions in vivo. *J Appl Physiol* 95: 829–837, 2003.
31. **Flahiff CM, Brooks AT, Hollis JM, Vander Schilden JL, Nicholas RW.** Biomechanical analysis of patellar tendon allografts as a function of donor age. *Am J Sports Med* 23: 354–358, 1995.
32. **Frank C, McDonald D, Wilson J, Eyre D, Shrive N.** Rabbit medial collateral ligament scar weakness is associated with decreased collagen pyridinoline crosslink density. *J Orthop Res* 13: 157–165, 1995.
33. **Fukashiro S, Itoh M, Ichinose Y, Kawakami Y, Fukunaga T.** Ultrasonography gives directly but noninvasively elastic characteristic of human tendon in vivo. *Eur J Appl Physiol Occup Physiol* 71: 555–557, 1995.
34. **Galeski A, Kastelic J, Baer E, Kohn RR.** Mechanical and structural changes in rat tail tendon induced by alloxan diabetes and aging. *J Biomech* 10: 775–782, 1977.
35. **Hannukainen J, Kalliokoski KK, Nuutila P, Fujimoto T, Kemppainen J, Viljanen T, Laaksonen MS, Parkkola R, Knuuti J, Kjaer M.** In vivo measurements of glucose uptake in human Achilles tendon during different exercise intensities. *Int J Sports Med* 26: 727–731, 2005.
36. **Hansen M, Kongsgaard M, Holm L, Skovgaard D, Magnusson SP, Qvortrup K, Larsen JO, Dahl M, Serup A, Frystyk J, Flyvbjerg A, Langberg H, Kjaer M.** Effect of estrogen on tendon collagen synthesis, tendon structural characteristics, and biomechanical properties in postmenopausal women. *J Appl Physiol* 106: 1385–1393, 2009.
37. **Hansen P, Bojsen-Moller J, Aagaard P, Kjaer M, Magnusson SP.** Mechanical properties of the human patellar tendon, in vivo. *Clin Biomech (Bristol, Avon)* 21: 54–58, 2006.
38. **Haus JM, Carrithers JA, Trappe SW, Trappe TA.** Collagen, cross-linking, and advanced glycation end products in aging human skeletal muscle. *J Appl Physiol* 103: 2068–2076, 2007.
39. **Haut RC, Lancaster RL, DeCamp CE.** Mechanical properties of the canine patellar tendon: some correlations with age and the content of collagen. *J Biomech* 25: 163–173, 1992.
40. **Hubbard RP, Soutas-Little RW.** Mechanical properties of human tendon and their age dependence. *J Biomech Eng* 106: 144–150, 1984.
41. **Johnson GA, Tramaglini DM, Levine RE, Ohno K, Choi NY, Woo SL.** Tensile and viscoelastic properties of human patellar tendon. *J Orthop Res* 12: 796–803, 1994.
42. **Kalliokoski KK, Langberg H, Ryberg AK, Scheede-Bergdahl C, Doessing S, Kjaer A, Boushel R, Kjaer M.** The effect of dynamic knee-extension exercise on patellar tendon and quadriceps femoris muscle glucose uptake in humans studied by positron emission tomography. *J Appl Physiol* 99: 1189–1192, 2005.
43. **Karamanidis K, Arampatzis A.** Mechanical and morphological properties of human quadriceps femoris and triceps surae muscle-tendon unit in relation to aging and running. *J Biomech* 39: 406–417, 2006.
44. **Kjaer M.** Role of extracellular matrix in adaptation of tendon and skeletal muscle to mechanical loading. *Physiol Rev* 84: 649–698, 2004.
45. **Kongsgaard M, Kovanen V, Aagaard P, Doessing S, Hansen P, Kjaer M, Magnusson SP.** Peritendinous corticosteroid injections, eccentric decline squat training and heavy slow resistance training in patellar tendinopathy. *Scand J Med Sci Sports* In press.
46. **Kongsgaard M, Reitelseder S, Pedersen TG, Holm L, Aagaard P, Kjaer M, Magnusson SP.** Region specific patellar tendon hypertrophy in humans following resistance training. *Acta Physiol (Oxf)* 191: 111–121, 2007.
47. **Kubo K, Ishida Y, Komuro T, Tsunoda N, Kanehisa H, Fukunaga T.** Age-related differences in the force generation capabilities and tendon extensibilities of knee extensors and plantar flexors in men. *J Gerontol A Biol Sci Med Sci* 62: 1252–1258, 2007.
48. **Kubo K, Kanehisa H, Miyatani M, Tachi M, Fukunaga T.** Effect of low-load resistance training on the tendon properties in middle-aged and elderly women. *Acta Physiol Scand* 178: 25–32, 2003.
49. **Kubo K, Morimoto M, Komuro T, Tsunoda N, Kanehisa H, Fukunaga T.** Age-related differences in the properties of the plantar flexor muscles and tendons. *Med Sci Sports Exerc* 39: 541–547, 2007.
50. **Langberg H, Rosendal L, Kjaer M.** Training-induced changes in peritendinous type I collagen turnover determined by microdialysis in humans. *J Physiol* 534: 297–302, 2001.
51. **Langberg H, Skovgaard D, Petersen LJ, Bulow J, Kjaer M.** Type I collagen synthesis and degradation in peritendinous tissue after exercise determined by microdialysis in humans. *J Physiol* 521: 299–306, 1999.
52. **Mademli L, Arampatzis A, Walsh M.** Age-related effect of static and cyclic loadings on the strain-force curve of the vastus lateralis tendon and aponeurosis. *J Biomech Eng* 130: 011007, 2008.
53. **Maganaris CN, Paul JP.** In vivo human tendon mechanical properties. *J Physiol* 521: 307–313, 1999.

Downloaded from on April 7, 2015

54. **Magnusson SP, Aagaard P, Dyhre-Poulsen P, Kjaer M.** Load-displacement properties of the human triceps surae aponeurosis in vivo. *J Physiol* 531: 277–288, 2001.
55. **Magnusson SP, Beyer N, Abrahamsen H, Aagaard P, Neergaard K, Kjaer M.** Increased cross-sectional area and reduced tensile stress of the Achilles tendon in elderly compared with young women. *J Gerontol A Biol Sci Med Sci* 58: 123–127, 2003.
56. **Magnusson SP, Hansen M, Langberg H, Miller B, Haraldsson B, Westh EK, Koskinen S, Aagaard P, Kjaer M.** The adaptability of tendon to loading differs in men and women. *Int J Exp Pathol* 88: 237–240, 2007.
57. **Magnusson SP, Hansen P, Aagaard P, Brond J, Dyhre-Poulsen P, Bojsen-Moller J, Kjaer M.** Differential strain patterns of the human gastrocnemius aponeurosis and free tendon, in vivo. *Acta Physiol Scand* 177: 185–195, 2003.
58. **Magnusson SP, Narici MV, Maganaris CN, Kjaer M.** Human tendon behaviour and adaptation, in vivo. *J Physiol* 586: 71–81, 2008.
59. **Maillard L.** Action des acides aminés sur les sucres: formation des mélanoïdines par voie méthodique. *C R Acad Sci* 154: 66–68, 1912.
60. **Markovic G, Jaric S.** Movement performance and body size: the relationship for different groups of tests. *Eur J Appl Physiol* 92: 139–149, 2004.
61. **Mian OS, Thom JM, Ardigo LP, Minetti AE, Narici MV.** Gastrocnemius muscle-tendon behaviour during walking in young and older adults. *Acta Physiol (Oxf)* 189: 57–65, 2007.
62. **Monnier VM.** Toward a Maillard reaction theory of aging. *Prog Clin Biol Res* 304: 1–22, 1989.
63. **Morse CI, Thom JM, Birch KM, Narici MV.** Tendon elongation influences the amplitude of interpolated doublets in the assessment of activation in elderly men. *J Appl Physiol* 98: 221–226, 2005.
64. **Munch G, Schinzel R, Loske C, Wong A, Durany N, Li JJ, Vlassara H, Smith MA, Perry G, Riederer P.** Alzheimer's disease—synergistic effects of glucose deficit, oxidative stress and advanced glycation end-products. *J Neural Transm* 105: 439–461, 1998.
65. **Nakagawa Y, Majima T, Nagashima K.** Effect of ageing on ultrastructure of slow and fast skeletal muscle tendon in rabbit Achilles tendons. *Acta Physiol Scand* 152: 307–313, 1994.
66. **Narici MV, Maganaris C, Reeves N.** Myotendinous alterations and effects of resistive loading in old age. *Scand J Med Sci Sports* 15: 392–401, 2005.
67. **Narici MV, Maganaris CN.** Plasticity of the muscle-tendon complex with disuse and aging. *Exerc Sport Sci Rev* 35: 126–134, 2007.
68. **Ng GY, Oakes BW, Deacon OW, McLean ID, Eyre DR.** Long-term study of the biochemistry and biomechanics of anterior cruciate ligament-patellar tendon autografts in goats. *J Orthop Res* 14: 851–856, 1996.
69. **Nielsen HM, Skalicky M, Viidik A.** Influence of physical exercise on aging rats. III. Life-long exercise modifies the aging changes of the mechanical properties of limb muscle tendons. *Mech Ageing Dev* 100: 243–260, 1998.
70. **Onambele GL, Narici MV, Maganaris CN.** Calf muscle-tendon properties and postural balance in old age. *J Appl Physiol* 100: 2048–2056, 2006.
71. **Onambele GN, Burgess K, Pearson SJ.** Gender-specific in vivo measurement of the structural and mechanical properties of the human patellar tendon. *J Orthop Res* 25: 1635–1642, 2007.
72. **Oxlund H, Barckman M, Ortoft G, Andreassen TT.** Reduced concentrations of collagen cross-links are associated with reduced strength of bone. *Bone* 17: 365S–371S, 1995.
73. **Parry DA.** The molecular and fibrillar structure of collagen and its relationship to the mechanical properties of connective tissue. *Biophys Chem* 29: 195–209, 1988.
74. **Parry DA, Barnes GR, Craig AS.** A comparison of the size distribution of collagen fibrils in connective tissues as a function of age and a possible relation between fibril size distribution and mechanical properties. *Proc R Soc Lond B Biol Sci* 203: 305–321, 1978.
75. **Partington FR, Wood GC.** The role of non-collagen components in the mechanical behaviour of tendon fibres. *Biochim Biophys Acta* 69: 485–495, 1963.
76. **Patterson-Kane JC, Parry DA, Birch HL, Goodship AE, Firth EC.** An age-related study of morphology and cross-link composition of collagen fibrils in the digital flexor tendons of young thoroughbred horses. *Connect Tissue Res* 36: 253–260, 1997.
77. **Provenzano PP, Vanderby R Jr.** Collagen fibril morphology and organization: implications for force transmission in ligament and tendon. *Matrix Biol* 25: 71–84, 2006.
78. **Reddy GK.** Cross-linking in collagen by nonenzymatic glycation increases the matrix stiffness in rabbit achilles tendon. *Exp Diabesity Res* 5: 143–153, 2004.
79. **Reddy GK, Stehno-Bittel L, Enwemeka CS.** Glycation-induced matrix stability in the rabbit achilles tendon. *Arch Biochem Biophys* 399: 174–180, 2002.
80. **Reeves ND, Maganaris CN, Narici MV.** Effect of strength training on human patella tendon mechanical properties of older individuals. *J Physiol* 548: 971–981, 2003.
81. **Saito M, Marumo K, Fujii K, Ishioka N.** Single-column high-performance liquid chromatographic-fluorescence detection of immature, mature, and senescent cross-links of collagen. *Anal Biochem* 253: 26–32, 1997.
82. **Sargon MF, Ozlu K, Oken F.** Age-related changes in human tendo calcaneus collagen fibrils. *Saudi Med J* 26: 425–428, 2005.
83. **Shadwick RE.** Elastic energy storage in tendons: mechanical differences related to function and age. *J Appl Physiol* 68: 1033–1040, 1990.
84. **Suzuki D, Takahashi M, Abe M, Nagano A.** Biochemical study of collagen and its crosslinks in the anterior cruciate ligament and the tissues used as a graft for reconstruction of the anterior cruciate ligament. *Connect Tissue Res* 49: 42–47, 2008.
85. **Verzar F.** The aging of collagen. *Sci Am* 208: 104–114, 1963.
86. **Verzijl N, DeGroot J, Oldehinkel E, Bank RA, Thorpe SR, Baynes JW, Bayliss MT, Bijlsma JW, Lafeber FP, TeKoppele JM.** Age-related accumulation of Maillard reaction products in human articular cartilage collagen. *Biochem J* 350: 381–387, 2000.
87. **Visser JJ, Hoogkamer JE, Bobbert MF, Huijing PA.** Length and moment arm of human leg muscles as a function of knee and hip-joint angles. *Eur J Appl Physiol Occup Physiol* 61: 453–460, 1990.
88. **Vlassara H.** Advanced glycation end-products and atherosclerosis. *Ann Med* 28: 419–426, 1996.
89. **Vlassara H.** Protein glycation in the kidney: role in diabetes and aging. *Kidney Int* 49: 1795–1804, 1996.
90. **Vogel HG.** Influence of maturation and age on mechanical and biochemical parameters of connective tissue of various organs in the rat. *Connect Tissue Res* 6: 161–166, 1978.
91. **Vogel HG.** Age dependence of mechanical properties of rat tail tendons (hysteresis experiments). *Aktuelle Gerontol* 13: 22–27, 1983.

Downloaded from on April 7, 2015